# A STUDY OF THE FLUORESCENCE EXCITATION SPECTRUM OF CRYSTALLINE ANTHRACENE

by

ADRIAN STANFORD DRIVER B.Sc. Hons. (Rhodes)

A thesis presented for the degree of Master of Science of Rhodes University.

- - - - - - - - - - - - - - -

December, 1960.

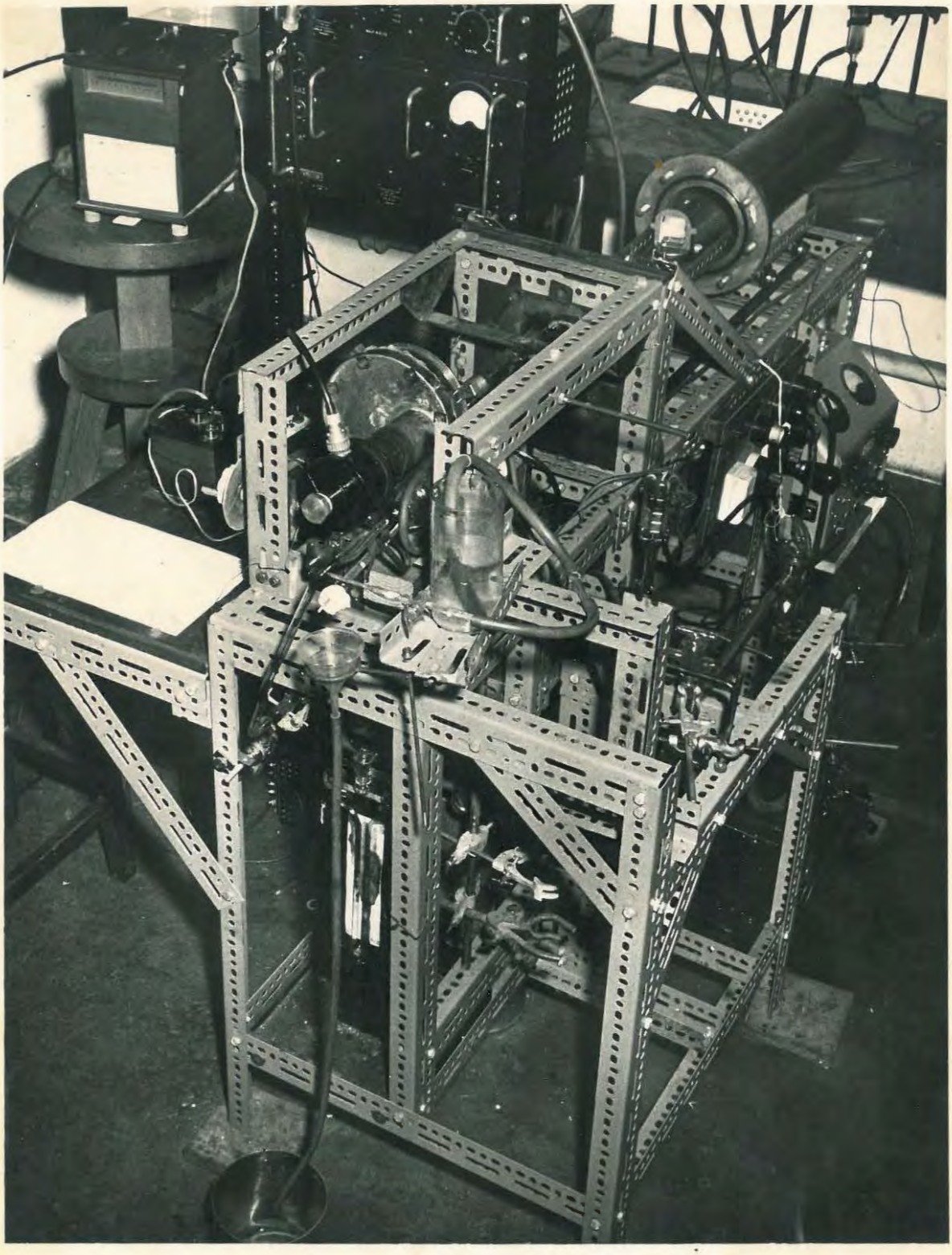

FRONTISPIECE THE VACUUM SPECTROGRAPH.

ACKNOWLEDGEMENTS.

The writer is greatly indebted to the following:

Professor J.A. Gledhill for supervising this work, and for his guidance and interest in the project; also for his helpful criticisms of a draft of the thesis.

The Council for Scientific and Industrial Research for a bursary held for two years.

The Council of Rhodes University for a grant used for maintenance of the spectograph.

Mr. A.R. Scanlen, Mr. G. Walters, Mr. F. Van de Water and Mr. J.W. West for their kind help and co-operation in glass-blowing, photography and engineering problems.

Mr. H. Eales of Rhodes University for assisting in the identification of crystal cleavage planes.

Mr. H.E.S. Driver and Mr. J.O.S. Driver for donating metals for making electrodes.

Dr. T.J. Hugo for the gift of quartz discs.

Mr. T.M. Allan for zerographing some of the diagrams.

* * * * *

- C O N T E N T S -

Page.

# CHAPTER I.

## INTRODUCTION.

The work described in this thesis was performed at the Physics Department, Rhodes University during 1958 and 1959 under the supervision of Professor J.A. Gledhill. Use was made of a vacuum ultra-violet spectrograph which had been constructed in the Physics Department (1.1), and modifications to be described were made to this instrument. The instrument was used for studying the effects of oxygen on the fluorescence excitation spectrum of Anthracene.

## FLUORESCENCE EXCITATION SPECTRA

If radiation of a certain wavelength is absorbed by molecules of a substance and is then emitted within $10^{-8}$ sec. by the molecules as radiation of a longer wavelength, the substance may be said to have the property of fluorescence. The energy yield of the substance may be defined as the ratio of the energy of the secondary radiation (fluorescence) to the energy of the primary (absorbed) radiation (1.2). The energy of radiation may be measured by the flow of energy per second, or by the flow of the number of quanta of the radiation per second through a unit surface area perpendicular to the direction of flow. If the energies of the primary and secondary radiations are measured in energy units, the ratio will be the energy yield G. If they are measured by the number of quanta, the ratio will be the quantum efficiency B.

If $\nu_a$ and $\nu_e$ are frequencies of absorbed and emitted quanta, $N(\nu)$ is the number of quanta of frequency $\nu$, and h is Planck's constant, then

$$G = \frac{N(\nu_e)h\nu_e}{N(\nu_a)h\nu_a} \quad \text{and} \quad B = \frac{N(\nu_e)}{N(\nu_a)}$$

In general, $\nu_e$ is greater than $\nu_a$ (Stoke's Law).

If the ratio of the quantum efficiencies of two substances excited by the same monochromatic radiation is measured as a function of the frequency of the radiation, the relative fluorescence excitation spectrum of the substances is obtained. If the quantum efficiency of one of these substances is known to be independent of frequency, the relative excitation spectrum will be a measure of the frequency variation of the quantum efficiency of the other, i.e. a measure of the fluorescence excitation spectrum. Relative excitation spectra are easier to measure than the absolute spectra because the absolute values of quantum efficiencies are not easily measured (1.3). The method of measurement of relative excitation spectra will be described in Chapter III.

PREVIOUS WORK

The fluorescence excitation spectrum of single Anthracene crystals has been investigated for exciting wavelengths

between 900A and 4000A (1.3, 1.4, 1.5). The effect on the intensity of the spectrum of the length of exposure of the crystals to atmospheric air has also been investigated (1.3). It has been noted that minima in the excitation spectrum are related to maxima in the absorption spectrum between the wavelengths 3200A and 4000A (1.4).

PURPOSE OF THE INVESTIGATIONS

The effect of atmospheric oxygen on the fluorescence excitation spectrum of Anthracene crystals was to be studied. It was proposed to cleave an Anthracene crystal in a vacuum, and it was hoped to observe the spectrum before atmospheric oxygen combined with molecules on the newly cleaved surface on to which the exciting radiation was allowed to fall. It was also hoped that information about the relation between the wavelengths of absorption maxima and excitation minima in the vacuum ultraviolet region would be obtained.

EXCITATION SPECTRA AND EXCITATION

Pringsheim states that there is no spectral selectivity in the exciting power of the primary radiation (1.6). Apparent selectivity disappears if the apparent fluorescent intensities are corrected to values corresponding to equal energies absorbed by the fluorescent substance. Pringsheim was considering fluorescent dye solutions in regions of low absorption where not all

the primary energy was absorbed. Different amounts of energy penetrated through the sample, depending on the variation of the absorption coefficient with wavelength.

Molecules of a fluorescent substance may be excited by ultra-violet radiation to the first or higher electronic states, depending on the wavelength of the radiation. The excited molecules then lose some of their excess energy as heat, and by some process, they reach the lowest vibrational level of the first excited state. Thereafter, the molecules return to the ground state with the emission of fluorescence, and no fluorescence emission from fluorescent substances other than that resulting from electronic transitions between the first excited and ground states has been observed (1.6).

Pringsheim noted that the constancy of quantum efficiency for exciting light of all wavelengths smaller than those of the fluorescence band had been proved for numerous substances (1.6), and that quantum efficiences could be independent of the wavelength of the exciting radiation over regions corresponding to transitions to electronic states higher than the first in the absorption spectrum.

He therefore suggested that, since a second fluorescence band

Bowen states "The wavelength of the exciting light is usually without influence on the fluorescent intensity or colour, except in so far as the former is affected by differences in strength of light absorption" (1.9). He was referring to the fluorescence of solutions and it is presumed that he meant the excitation spectrum would vanish if corrected for equal amounts of absorbed energy.

An empirical law of Vavilov which was established for the fluorescence of molecular solutions, implies that the quantum yield of fluorescence is constant in the Stokes region of the spectrum, and falls rapidly in the anti-Stokes region (1.2, 1.10). (The latter region lies between the principal absorption and fluorescence bands). Verification of the law has also been claimed for inorganic crystalline phosphors (1.11). Because the accuracy of many early quantum efficiency measurements was limited, and measurements were usually made at large wavelength intervals, it is possible that variations in the excitation spectra were overlooked.

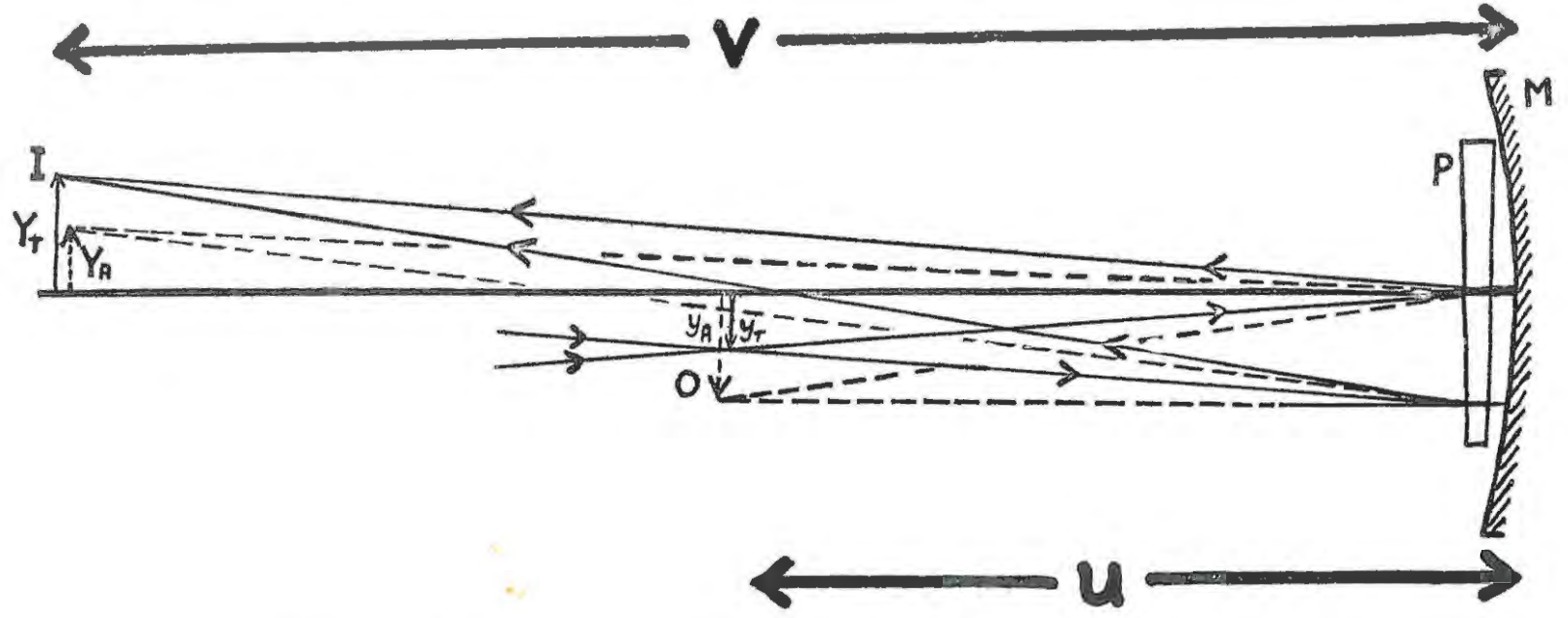


DIAGRAM 2.1 OPTICAL PRINCIPLE

## CHAPTER II

## DESCRIPTION OF THE SPECTROGRAPH.

The instrument used for making measurements of excitation spectra of Anthracene crystals was a prism spectrograph constructed for use in the far and vacuum ultra-violet regions of the spectrum between the wavelengths 1300A and 3000A (1.1).

The contributions of the writer to the instrument were:

1. Minor alterations to the design,
2. Construction of a crystal cleaving attachment (Chapter III).

### OPTICAL SYSTEM

The optical principle is illustrated in Diagram 2.1. The image of an illuminated slit situated at a distance u in front of a concave aluminised mirror M was brought to a focus at a distance v from the mirror. A wedge-shaped Calcium Fluoride prism P having a small refracting angle was introduced immediately in front of the mirror with its refracting edge parallel to the slit. The prism deviated the paths of all rays of light passing through it through a small angle, and therefore the image of the slit was shifted slightly. Because the prism deviated rays of different wavelengths through different angles, the image was spectrally dispersed. A

second slit, parallel to the first, and fixed relative to it, was situated where the spectrally dispersed image came to a focus. The prism and mirror were fixed relative to each other, and could be rotated about a vertical axis parallel to the slits and passing through the pole of the mirror. The wavelength of light passing through the second or exit slit of the spectrograph was varied by rotating the prism and mirror through small angles so that different sections of the spectrally dispersed image fell on the exit slit.

The mirror had been aluminised because Aluminium has one of the highest reflectivities in the vacuum ultra-violet region (2.1), and the prism was made of pure Calcium Fluoride which is transparent to radiation of wavelength longer than 1250A.

It was desirable that light passing through the exit slit did not become unfocussed as the prism and mirror rotated. A thin prism had therefore been chosen rather than a thick one in order that the distance from the pole of the mirror to the spectrally dispersed image should not vary appreciably with wavelength.

Details of the optical system

| | |
|---|---|
| Distance of entrance slit from mirror (u) | : 40cm. (approx.) |
| Distance of exit slit from mirror (v) | : 80cm. " |
| Focal length of mirror | : 28.1cm. |
| Width of entrance slit | : .040mm. |
| Width of exit slit | : .065mm. |
| Angle of prism | : 5° |
| Size of refracting faces of prism | : 4cm. x 4cm. |

## CALCULATION OF THE LINEAR DISPERSION OF THE SPECTRUM AT THE EXIT SLIT.

Diagram 2.1 represents the formation by monochromatic rays of an image of the entrance slit of the spectrograph. The unbroken lines representing rays show the actual paths of two particular rays between the slit at O and the image at I. The broken lines represent the extensions of the paths of these rays in the space between the prism and mirror. A line was drawn bisecting the angle between the broken lines representing the extensions of the paths of that ray from the entrance slit reflected at the pole of the mirror. This line was chosen as a reference axis. The other ray from the entrance slit was chosen so that its path was parallel to the reference axis after having passed through the prism once. The distances of the entrance slit, its image, and the points of intersection of the broken lines from the reference axis are labelled $y_T$, $Y_T$, $y_A$, $Y_A$ as in Diagram 2.1. A ray incident at a small angle on a thin prism in a plane perpendicular to its refracting edge will be deviated through an angle $A(\mu-1)$ on passing through the prism. A is the refracting angle of the prism, and $\mu$ is the refractive index of the material of the prism for the wavelength of the ray. From diagram 2.1 it follows that

$$y_A = y_T + A(\mu-1)U \qquad \ldots\ldots\ldots \quad (1)$$

$$Y_A = Y_T - A(\mu-1)V \qquad \ldots\ldots\ldots \quad (2)$$

TABLE I.

Dispersion = $2AV \frac{d\mu}{d\lambda}$

| Wavelength (A) | 3000 | 2500 | 2000 | 1600 | 1500 | 1400 |
|---|---|---|---|---|---|---|
| Dispersion mm/A x $10^3$ | 2·8 | 5·2 | 11·5 | 32 | 40 | 67 |
| Reciprocal Dispersion A/mm. | 360 | 190 | 87 | 31 | 25 | 15 |

From the laws of reflection it follows that:

$$\frac{y_A}{u} = \frac{Y_A}{v} \qquad \ldots\ldots\ldots (3)$$

The linear dispersion of the spectrum will be defined as the rate of change of its wavelength with distance in a plane perpendicular to the refracting edge of the prism and the entrance slit when the latter is fixed relative to the mirror.

i.e. Linear dispersion $= \left(\frac{\partial Y_T}{\partial \lambda}\right)_{y_T}$

It follows that Linear dispersion $= \left(\frac{\partial Y_T}{\partial \mu}\right)_{y_T} \left(\frac{\partial \mu}{\partial \lambda}\right)_{y_T}$

$$= \left(Av + \frac{\partial Y_A}{\partial \mu}\right)_{y_T} \frac{d\mu}{d\lambda}$$

$$= \left(Av + \frac{v}{u}\frac{\partial y_A}{\partial \mu}\right)_{y_T} \frac{d\mu}{d\lambda}$$

$$= 2Av \frac{d\mu}{d\lambda} \qquad \ldots\ldots\ldots (4)$$

The refractive indices of Calcium Fluoride for various wavelengths are listed in tables (2.2). From these tables, values of $\frac{d\mu}{d\lambda}$ were evaluated which were used to find the linear dispersion of the spectrum at various wavelengths. The results are given in Table I.

THE RADIATION SOURCE

An electrical discharge through Hydrogen gas at a pressure of a few millimeters of Mercury excites a continuous ultra-violet spectrum which was utilised for measurement of fluorescence excitation spectra. The spectrum was excited in a capillary type, water-cooled Silica discharge tube. A cross-section of the tube is illustrated in Diagram 2.2. Radiation passed through one of the cylindrical electrodes and the Calcium Fluoride window at one end in its passage from the capillary to the entrance slit of the spectrograph.

Periodically the discharge tube was refilled with fresh hydrogen in order to reduce the risk of explosion of the hydrogen with atmospheric oxygen which may have leaked in. The interior of the tube was evacuated to a pressure of lower than $10^{-4}$mm. Hg. through tube A which was connected to a diffusion pump. The connection to the diffusion pump was then closed, and a small jet of burning Hydrogen was played on to the Palladium filling tube B. Within a few minutes, enough pure Hydrogen had diffused through the Palladium tube into the discharge tube to give a pressure of 10mm. Hg. (The method of measuring the pressure in the tube will be illustrated when the vacuum system is described.) Water was allowed to drip on to a wet piece of cotton wool draped around the metal-to-glass seal which connected the Palladium tube with the interior of the

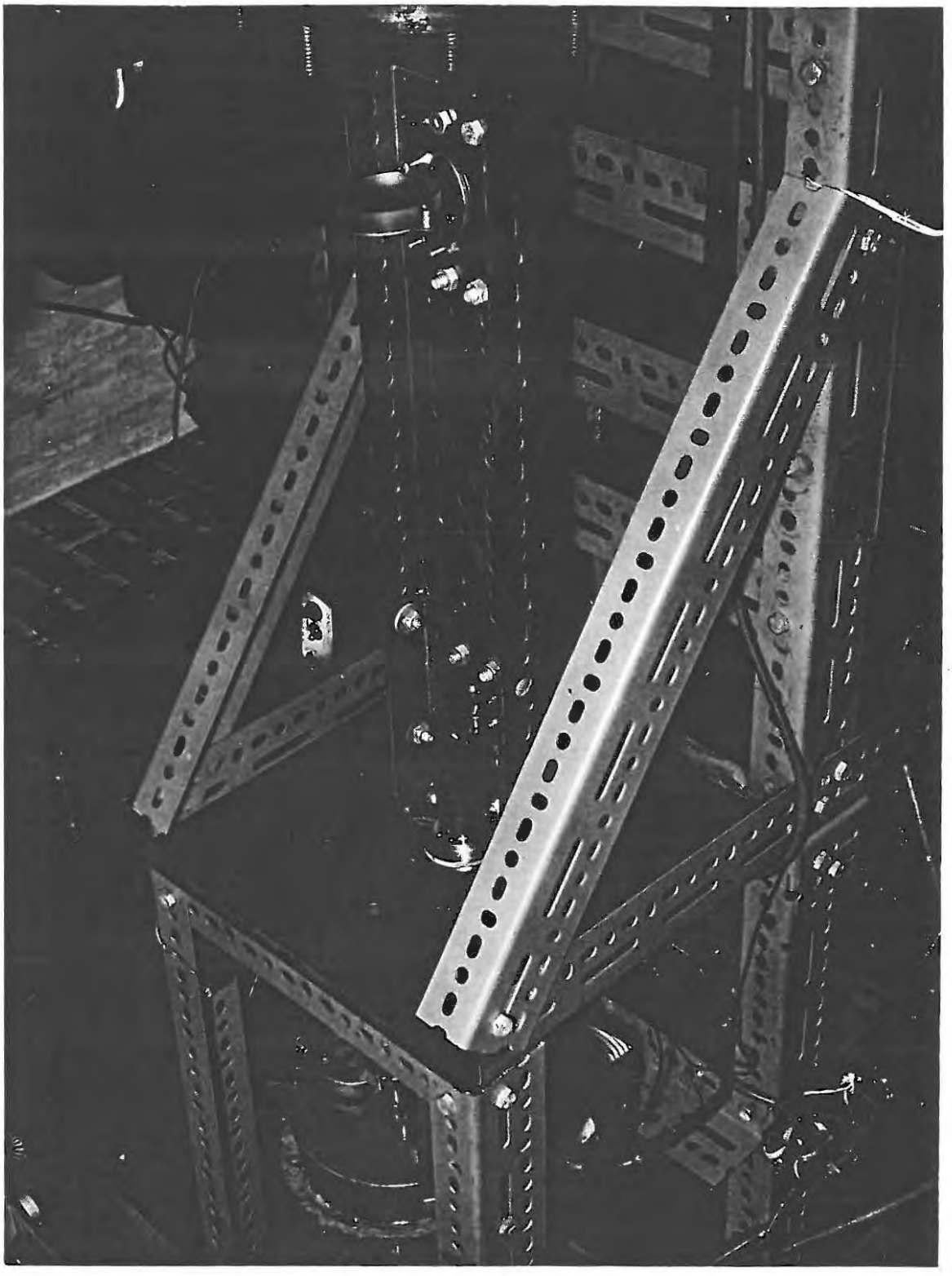

PLATE 1. ILLUSTRATION OF THE SPECTROGRAPH.

discharge tube. Heat which was conducted along the Palladium tube was prevented from cracking the seal in this way.

The discharge tube was run off a transformer capable of supplying a current of 500mA at a voltage of 4KV. The discharge current was limited to 320 mA by a resistance consisting of 8 x 250V 100W globes in series with the discharge tube. The circuit used for supplying the power for the discharge is illustrated in Diagram 2.2. The discharge current and the intensity of light given out from the tube were usually very steady. A device to ensure that the tube would be cooled while the discharge current was flowing is also illustrated in Diagram 2.2.

THE CONSTRUCTION OF THE SPECTROGRAPH

The construction of the spectrograph is illustrated by the frontispiece, Plate I, and Diagrams 2.3, 2.4, 2.5, 2.6, 2.7.

The prism and mirror were mounted on a horizontal table which was rotatable about a vertical axis passing through the pole of the mirror. This table and the entrance slit of the spectrograph were mounted on a horizontal cantilever which was joined at one end to a vertical steel base plate (See Plate I and Diagram 2.3). A metal pipe closed at one end formed the main vacuum chamber. A flange at the open end

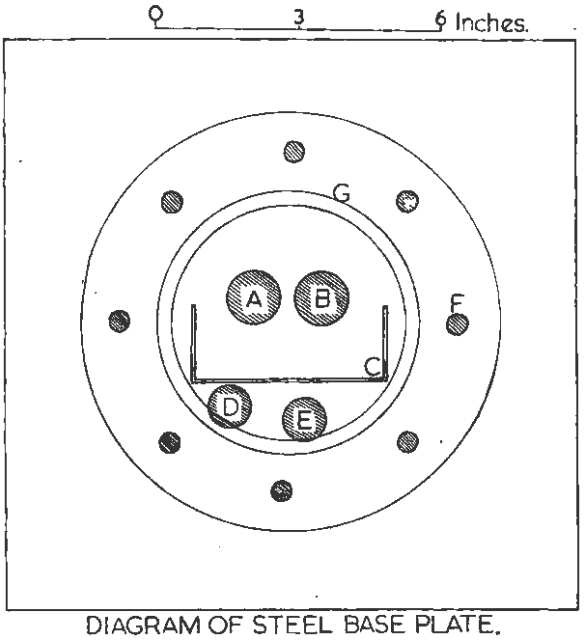


DIAGRAM OF STEEL BASE PLATE.

A,B. Holes for passage of radiation.
C. Position of cantilever.
D. To diffusion pump.
E. Hole for rotary transmission.
F. Holes for bolts.
G. Position of steel pipe.

DIAGRAM 2.4

## DIAGRAM 2.2.

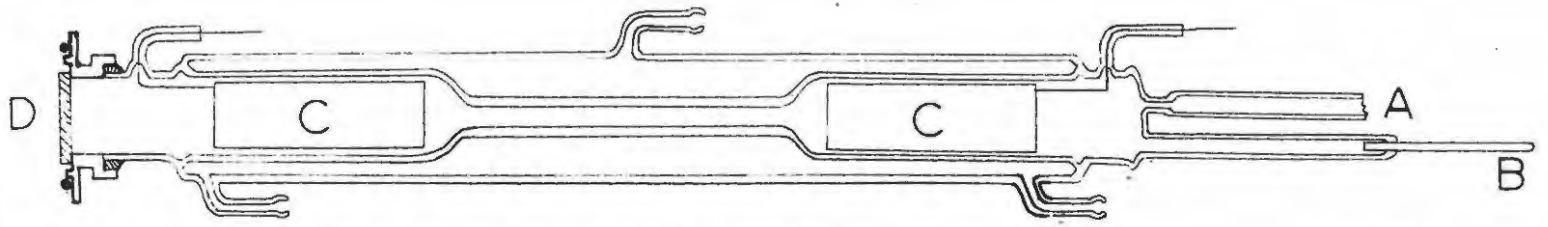


HYDROGEN DISCHARGE TUBE. 0 10 CM

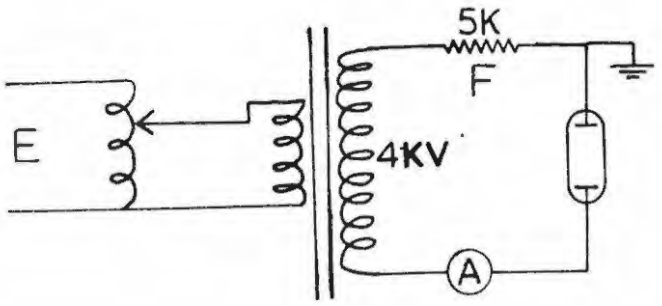


DISCHARGE TUBE ELECTRICAL SYSTEM.

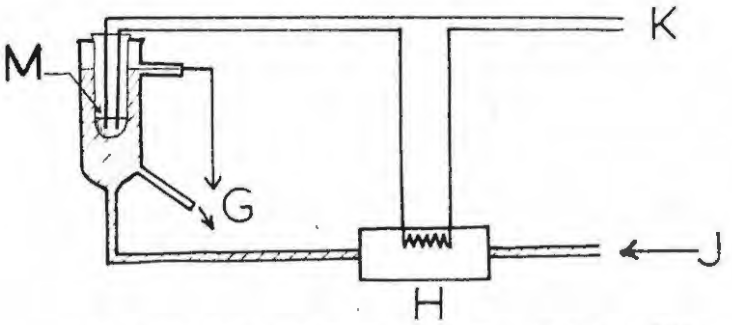


SAFETY COOLING DEVICE

A To high vacuum system.
B Palladium filling tube.
C Aluminium electrodes.
D Calcium fluoride window.
E Variac.
F Resistance in form of 8×100W 250V globes
G Water outlet.
H Device to be cooled.
J Flow of cooling water from tap.
K Electrical power circiut.
M Mercury in floating test tube

A To radiation source.
B Flexible metal bellows.
C HILGER adjustable calibrated slit.
D Knurled ring for adjusting slit width.
E Screw for adjustment of position of C.
F Prism table.
G Fluorite prism.
H Concave aluminised mirror.
J End of cantilever.
K Baffle.
L To exit slit and crystal cleaving device.
M Screws for leveling prism table.

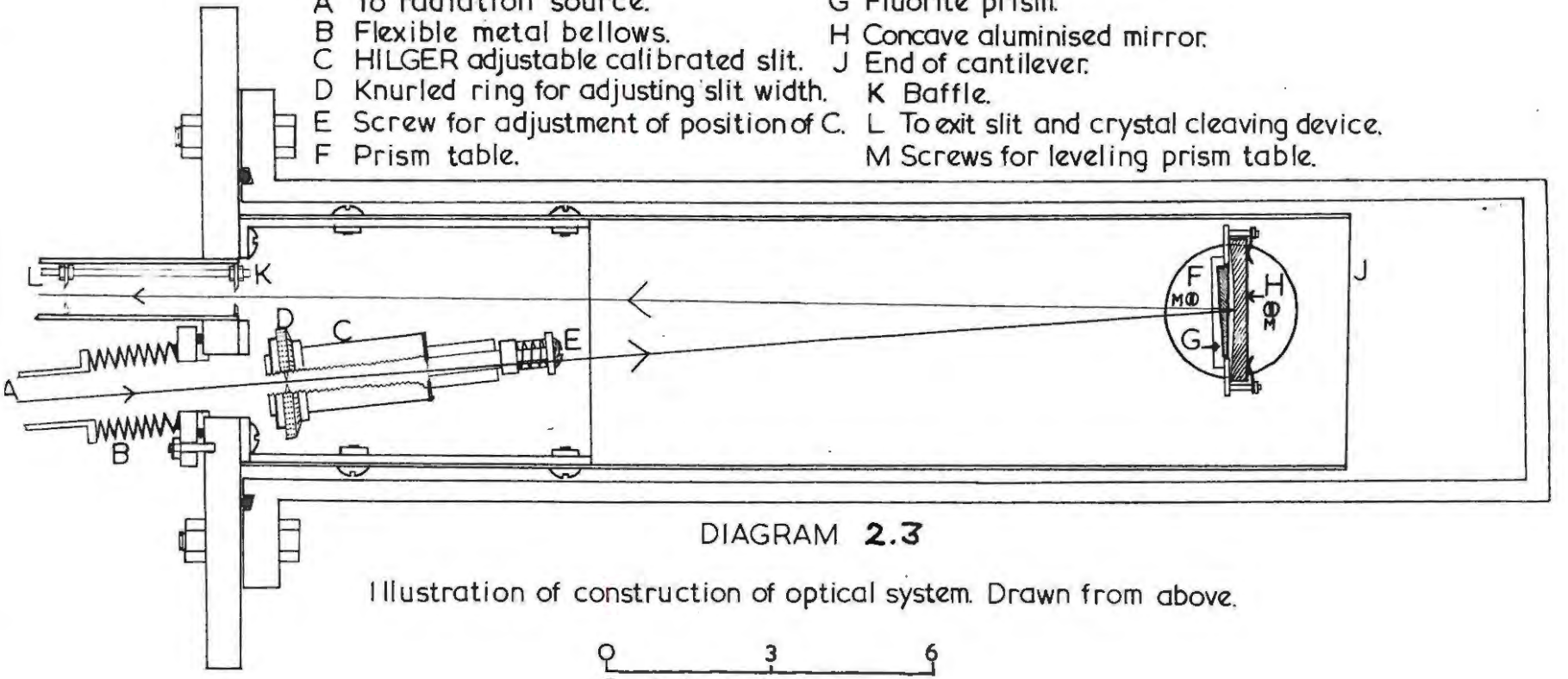


DIAGRAM **2.3**

Illustration of construction of optical system. Drawn from above.

0 3 6

Scale in inches.

of the pipe was bolted against an O-ring to the vertical steel base plate so that the cantilever was enclosed by the pipe. Access to the interior of the main vacuum chamber was readily obtained by unbolting the flange and removing the steel pipe.

A cross-section of the base plate is illustrated in Diagram 2.4. Radiation from the discharge tube passed through hole A in the steel base plate to the entrance slit in the main vacuum chamber. After reflection at the mirror, the radiation passed out of the main vacuum chamber again through a second hole B in the steel base plate before coming to a focus at the exit slit. The exit slit was mounted at one end of a metal tube, the other end of which was soldered into the hole B. The crystal cleaving device which was attached to this tube at the end at which the exit slit was mounted, will be described in Chapter III.

THE MECHANISM FOR ROTATING THE TABLE

The table on which the prism and mirror were mounted had to be rotated through an angle of less than $2^{o}$ in order for the wavelength of the spectrum passing through the exit slit to change from 6000A to 1300A. As it was necessary for the wavelength to be continuously variable, the rotation of the table had to be finely controlled. This fine control was achieved

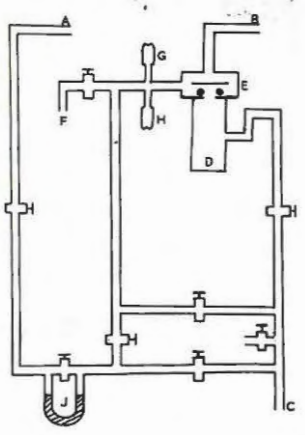


SCHEMATIC DIAGRAM OF VACUUM SYSTEM

A To discharge tube
B To spectrograph
C To mechanical pump
D Oil diffusion pump
E Plate valve
F To Macleod gauge
G Ionisation gauge
H Pirani gauge
J Oil manometer

**DIAGRAM 2.7**

by means of a mechanism situated beneath the cantilever in the main vacuum chamber. The mechanism is illustrated in Diagrams 2.5 and 2.6. It was operated from outside the vacuum by rotating about its own axis a shaft which passed directly into the vacuum through a "rotary transmission" screwed into a hole in the steel base plate. The mechanism was such that the rotation of the table was very nearly proportional to the rotation of this shaft.

A calculation showed that one complete revolution of the rotary transmission shaft effected a rotation of the table of 18.6 seconds of arc. The number of rotations N of the shaft were measured with a counter. In order to calibrate the spectrograph, it was necessary to know the values of N corresponding to the wavelengths at the exit slit. The accuracy with which given wavelengths were reproducible at the exit slit will be discussed in Chapter IV.

The exit slit and its mounting were removed, and the vizible spectrum of a light source placed in front of the entrance slit was observed with a microscope focussed in the plane in which the exit slit had been. The displacement of the spectrum in the field of view of the microscope was studied as a function of N, the rotation of the rotary transmission shaft. The smoothness with which the spectrum moved across the field of view as the rotary transmission shaft rotated was

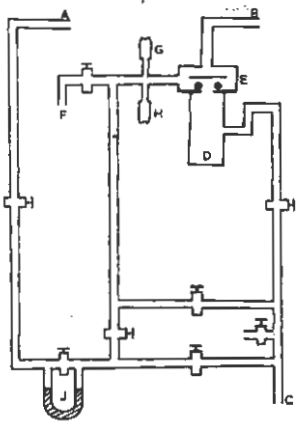


SCHEMATIC DIAGRAM OF VACUUM SYSTEM

A To discharge tube
B To spectrograph
C To mechanical pump
D Oil diffusion pump
E Plate valve
F To Macleod gauge
G Ionisation gauge
H Pirani gauge
J Oil manometer

**DIAGRAM 2.7**

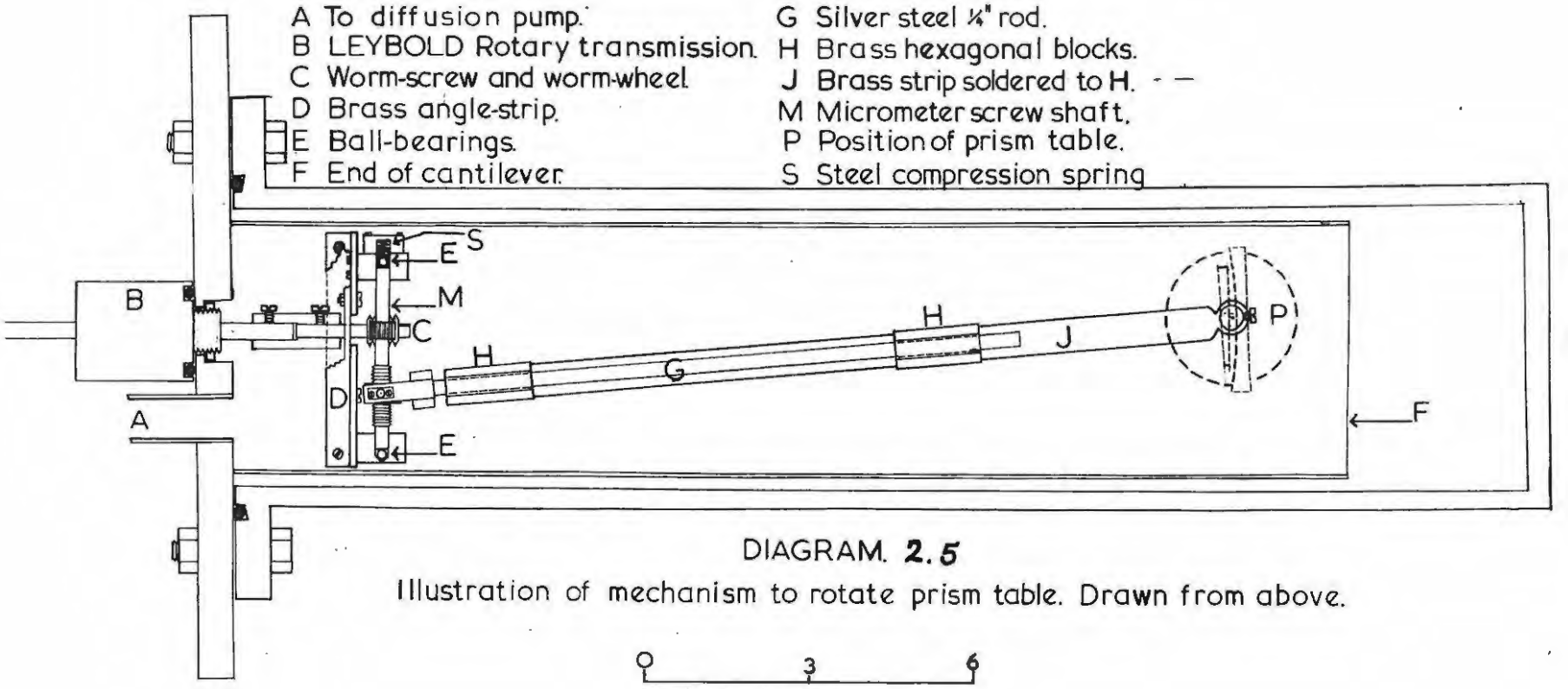


DIAGRAM. **2.5**

Illustration of mechanism to rotate prism table. Drawn from above.

A LEYBOLD rotary transmission.
B Micrometer screw shaft.
C Brass hexagon block.
D Prism table.
E Levelling screws.
F Calcium fluoride 5°thin prism.
G Concave aluminised mirror.
H Cantilever.
J HILGER calibrated adjustable slit.
K Screw for adjusting position of J.

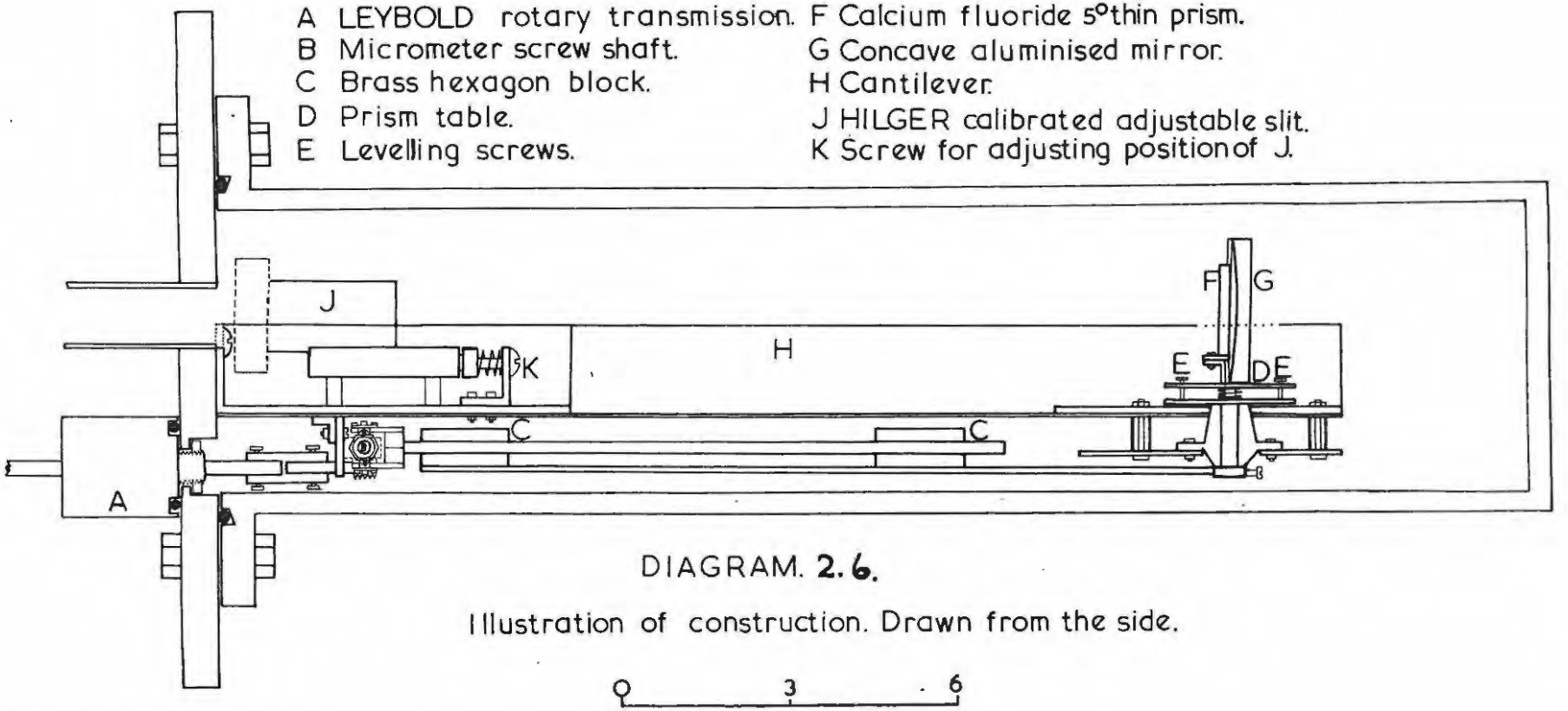


DIAGRAM. **2.6.**

Illustration of construction. Drawn from the side.

0 3 6

Scale in inches.

found by the writer to be satisfactory after minor alterations and adjustments to the mechanism which drove the table.

THE VACUUM SYSTEM

As air at atmospheric pressure absorbs ultra-violet radiation of wavelength shorter than 2200A strongly, it was necessary for the air in the spectrograph to be evacuated. Losses in intensity of the ultra-violet radiation as a result of absorption by air would be negligible if the vacuum pressure in the spectrograph was lower than $5 \times 10^{-4}$ mm. Hg. (2.3)

A scheme of the vacuum system is illustrated in Diagram 2.7. A mechanical pump attached at C was used to evacuate the spectrograph to a pressure of about $10^{-2}$ mm. Hg. Once this pressure had been reached, it was possible to bring into operation the oil diffusion pump D. The mechanical pump was also used to "back" the oil pump which reduced the pressure in the spectrograph from $10^{-2}$ mm. Hg. to about $5 \times 10^{-5}$ mm. Hg. usually within two hours.

The oil manometer J was used to measure the difference in pressure between the Hydrogen discharge tube and the high vacuum system. High vacuum oil having a suitably low vapour pressure was used to fill the arms of the manometer.

All O-rings and glass vacuum taps were greased with high vacuum grease, and were kept free of hairs and dust.

Vacuum pressures in the spectrograph were measured using Pirani and ionisation gauges. A McLeod gauge was used in order to check the accuracy of the vacuum pressures indicated by these gauges (G and H in Diagram 2.7). The lowest pressure obtained in the spectrograph was $10^{-5}$ mm. Hg.

ALIGNMENT OF THE OPTICAL SYSTEM

The exit slit of the spectrograph and its mounting were removed, and an ultra-violet quartz Mercury lamp was placed in front of the entrance slit. The vizible spectrum of the lamp was observed with a microscope focussed in the plane in which the exit slit had been. The entrance slit was rotated until the spectrum lines appeared to have the sharpest definition (when it would be parallel to the refracting edge of the prism). The exit slit and its mounting were then put back in position, and the microscope was focussed on the exit slit. The mounting was rotated until the slit appeared to be parallel to the edges of the spectrum lines which were seen in the microscope. The distance of the entrance slit from the prism was also adjusted for sharpest definition of the spectrum lines at the exit slit.

After these preliminary adjustments, the microscope was removed and a photomultiplier tube was placed so that its photosensitive cathode was opposite the exit slit. If the table was rotated so that the spectrum moved slowly past the exit slit, the intensity of light passing through the slit increased and

decreased again as each spectrum line moved across it. The correspomding variations in the photocurrent enabled the resolution of the spectrum lines to be studied. The spectrograph was judged to be well aligned optically if the Mercury spectrum line ringed in Diagram 4.1 (Chapter IV) was resolved as illustrated.

THE PHOTOMULTIPLIER TUBE

An RCA 6342 photomultiplier was found to be satisfactory for measuring light intensities at the exit slit on account of its low dark current (less than $10^{-2}\mu A$), its good stability, and its high amplification factor of the photocurrent produced at the cathode. The tube was always operated at its maximum anode voltage of 1500V, and the same tube was used for all measurements of photocurrents.

A galvanometer with a sensitivity of $1{\cdot}2 \times 10^{-3}\mu A/mm.$ was used in conjunction with a universal shunt to measure the photocurrent. The dark current of the photomultiplier was much reduced if the pins by means of which the tube was plugged into its base were clean. The dark current was found to become steady if a small quantity of Phosphoric acid drying agent was placed inside the casing which enclosed the photomultiplier.

SCATTERED LIGHT AND ITS REDUCTION

A bright light source was placed in front of the entrance

slit, and the steel pipe forming the main vacuum chamber was removed in order that spurious images and reflections from the prism and mirror could be studied. If the prism was rotated relative to the mirror through small angles about an axis parallel to its refracting edge, the beam of light which came to a focus at the exit slit to form the spectrum remained undeviated. The beams which gave rise to spurious images and reflections did not remain undeviated. The superposition of the images and reflections on the spectrum was avoided by carefully positioning the prism relative to the mirror.

The presence of spurious images and reflections would be expected to increase scattered light inside the spectrograph. Some of the scattered light would reach the exit slit. The greater proportion of scattered light would be of wavelength longer than 3000A, because the reflectivities of almost all substances decrease to low values for wavelengths in the far and vacuum ultra-violet regions.

A filter transparent to wavelengths longer than 3100A was placed opposite the exit slit, and the spectrograph was evacuated. The Hydrogen discharge was started, and a study was made of the scattered light transmitted by the filter when wavelengths of the Hydrogen spectrum between 1300A and 3000A passed through the exit slit. The scattered light was detected by means of a photomultiplier tube, and it was found

that the photocurrent did not exceed the value of $1.8 \times 10^{-3}$ μA. This photocurrent varied very gradually as the Hydrogen wavelengths passing through the exit slit changed. The possible effects of the presence of this scattered light on the relative fluorescence excitation spectra measured with this spectrograph will be discussed in Chapter III.

# CHAPTER III.

## THE CRYSTAL CLEAVING ATTACHMENT, AND MEASUREMENT OF SPECTRA.

The absorption coefficients of Anthracene for radiation having wavelengths in the far and vacuum ultra-violet regions of the spectrum are very high (3.1, 3.2), and such radiation incident on an Anthracene crystal will therefore be absorbed close to the surface. As radiation must be absorbed before fluorescence can take place, oxidation of the surface might be expected to affect the intensity of fluorescence. An attachment to the spectrograph was made which enabled a crystal inside a vacuum to be cleaved with a razor blade, so that the radiation which excited fluorescence could be allowed to fall on a newly formed surface of the crystal in an atmosphere as free of oxygen as possible. It was hoped to study changes in the intensity of fluorescence excitation spectra as the oxygen in the residual air in the vacuum combined with the molecules on the surface of the crystal.

### DESCRIPTION OF THE ATTACHMENT:

As explained in Chapter II, one end of the metal tube through which radiation passed in its passage from the prism to the exit slit of the spectrograph was soldered into one of the holes in the vertical steel base plate. The other end of the tube protruded for a distance of about three centimeters through a circular hole in the base of part of a 160 millimeter gunshell which was adapted for the construction of the cleaving attachment.

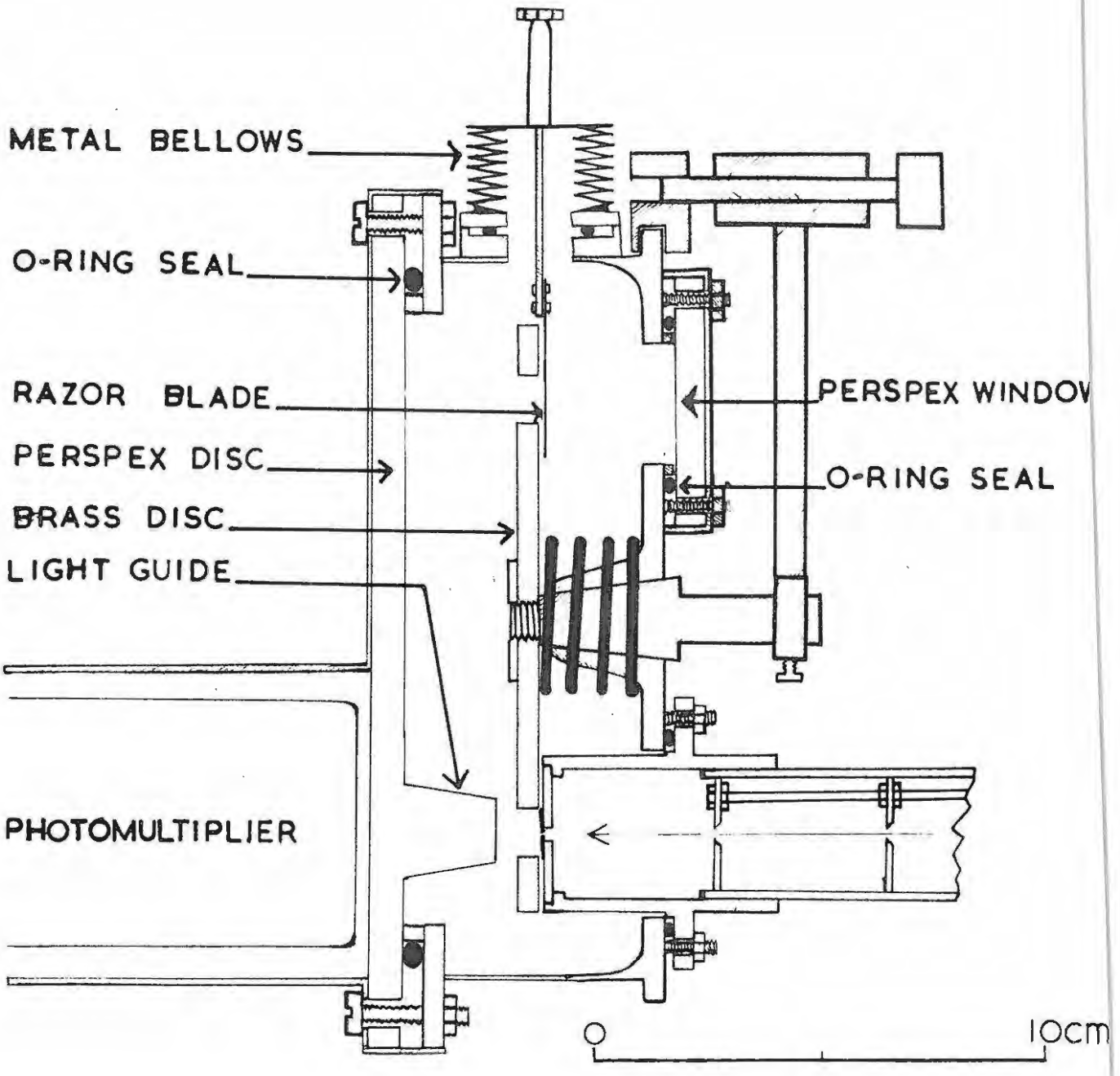


CRYSTAL CLEAVING DEVICE

DIAGRAM 3.1

A cross-section of the cleaving attachment is illustrated in Diagram 3.1. The shell was attached to the tube which protruded through its base by being bolted against an o-ring to a flange on the tube, as illustrated in the lower right of Diagram 3.1.

The arrow in Diagram 3.1 indicates the path of radiation to the exit slit through slots parallel to the exit slit in a row of baffle plates in the tube. The baffle plates prevented light which would be scattered by the inner walls of the tube from reaching the exit slit. Two razor blades were bolted to one face of a brass disc in such a way that their edges were opposite and parallel to each other, so that the exit slit was formed over a slot in the disc (Diagram 3.2). The disc itself was recessed into the end of the tube which protruded through the base of the shell.

The hole in the centre of the base of the shell where the percussion cap had been situated was made conical in shape, so that the larger diameter of the cone was on the outside of the shell. A conical piece of brass was ground into this hole, and the surfaces which had been ground together were greased with high vacuum grease. A thread was cut on the narrower end of the brass cone which protruded inside the shell, and a brass disc was screwed through its centre to the end of the brass cone, so that the faces of the disc were parallel to the base of the shell. Between the inside of the base of the shell and the brass disc, there was a steel compression spring, so that the brass cone would be kept pressed firmly into the conical cavity.

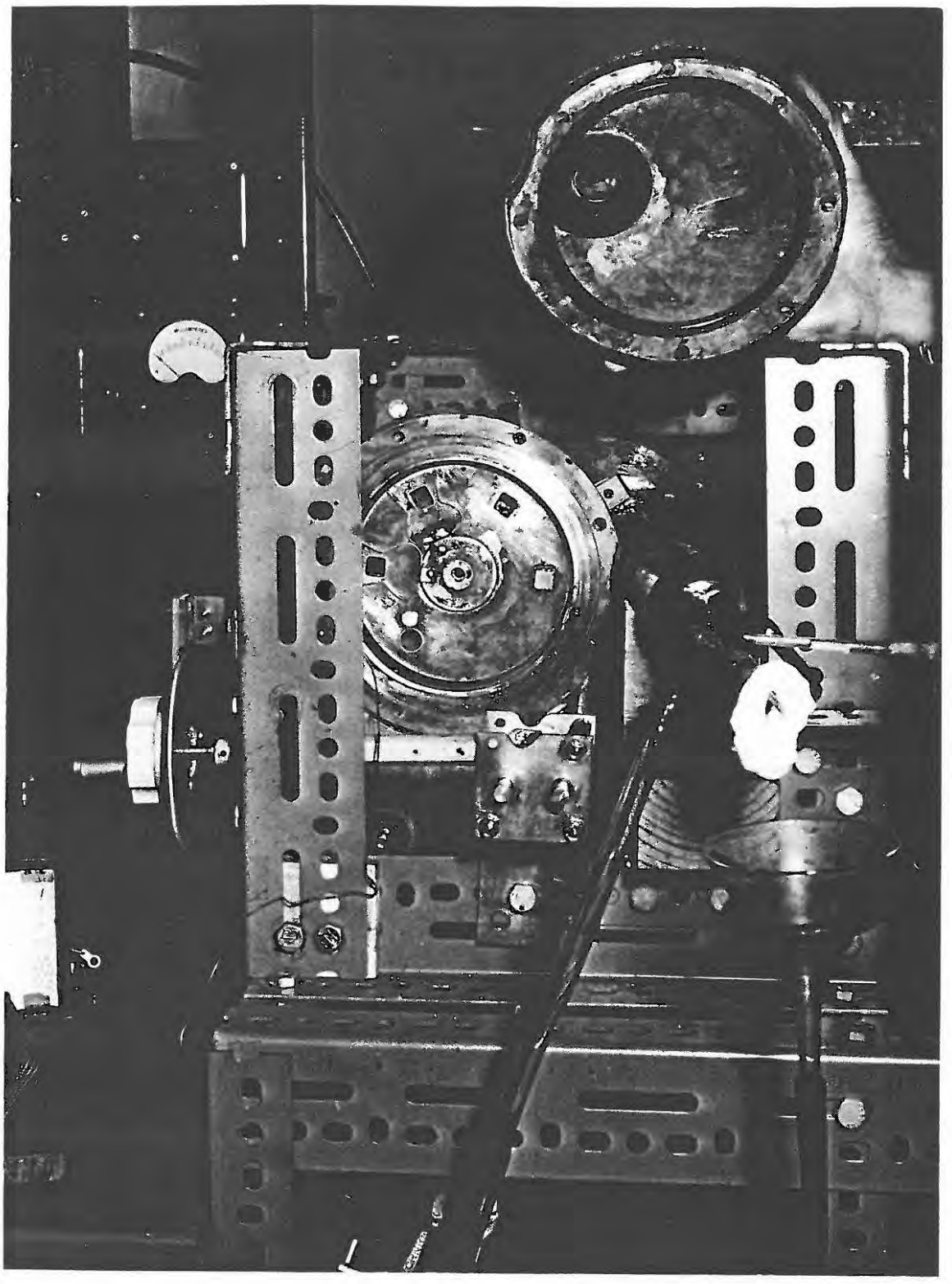

PLATE II: ILLUSTRATION SHOWING THE BRASS DISC IN THE INTERIOR OF THE CLEAVING CHAMBER.

EXIT SLIT

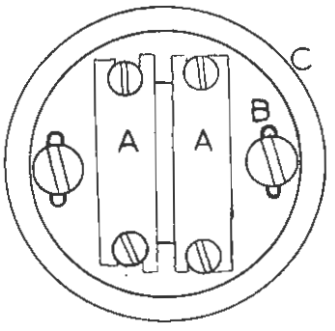


A Injector type razor blades.
B Brass disc.
C End of flange.

DIAGRAM 3.2

The crystals whose excitation spectra were to be investigated were in the shape of centimeter cubes, and there were holes in the disc slightly greater than one centimeter square for accommodating the crystals. The brass disc inside the shell is illustrated in Plate II.

There was a lever outside the cleaving chamber attached to the brass cone at right angles to its axis. By a manual rotation of the lever, the brass disc inside the shell could be rotated so that fluorescent specimens in the holes in the brass disc moved in turn in front of the exit slit. The disc could be fixed in any setting by means of the device at the further end of the lever from the centre of the shell. This device is illustrated in Diagram 3.1, and in Plate III, which shows the cleaving attachment in its position on the spectrograph.

The open end of the shell opposite the base was closed by means of a perspex disc which was bolted against an o-ring to a flange on the rim of the open end. The o-ring and the perspex disc may be seen in the upper right of Plate II. There was a perspex light guide joined to the perspex disc opposite the exit slit (Diagram 3.1). Fluorescence from specimens between the light guide and the exit slit passed through the light guide and the perspex disc to the photocathode of a photomultiplier situated outside the cleaving chamber and opposite the exit slit.

There were two holes in the cylindrical wall of the tube which supported the exit slit mounting inside the cleaving chamber, and when the spectrograph was evacuated, gas passed through these holes, down the tube

connecting the cleaving attachment with the spectrograph, to the main vacuum chamber and the vacuum pumps.

Inside the cleaving chamber, there was a razor blade which was joined to the end of a brass strip passing through a hole in the cylindrical wall of the shell. It is clear from Diagram 3.1 that the brass strip and the razor blade could be manoeuvred from outside the vacuum. The brass strip supported the razor blade parallel and close to the face of the brass disc nearest the base of the shell, and crystalline cubes of Anthracene to be cleaved were accommodated in the square holes in the disc so that they protruded from this face. When a vacuum had been obtained in the cleaving chamber, the brass disc was rotated until the crystal was opposite the razor blade, and the protruding part of the crystal was cleaved off. The cleaving operation could be watched from outside the vacuum through a window in the base of the shell. After the cleaving operation, the brass disc could be rotated through 180 degrees, so that the freshly cleaved face of the crystal was directly opposite the exit slit.

MEASUREMENT OF RELATIVE EXCITATION SPECTRA:

A thin layer of Sodium Salicylate was prepared on one face of a small quartz disc by evaporation of a dilute solution of Sodium Salicylate in distilled water from the disc. The quartz disc was glued with a non-fluorescent glue over one of the holes in the brass disc inside the cleaving chamber, and an Anthracene crystal was accommodated in another of the holes.

When the components of the cleaving chamber had been assembled, the air in the whole spectrograph, including the cleaving chamber, was evacuated until a vacuum pressure of lower than $10^{-4}$ mm. Hg. had been obtained. When the hydrogen discharge tube had been filled with hydrogen, the discharge was started, and the rotary transmission shaft which effected rotation of the prism table was rotated until ultra-violet radiation was passing through the exit slit.

A photomultiplier tube was placed opposite the exit slit as in Diagram 3.1, so that fluorescent light from specimens opposite the exit slit would fall on its photo-cathode. The brass disc in which fluorescent specimens were mounted was rotated from outside the vacuum, so that the Anthracene crystal and the Sodium Salicylate layer moved in turn opposite the exit slit, and the corresponding photo-currents were noted. From each of these currents was subtracted the dark current of the photomultiplier, which was the current measured when an opaque section of the brass disc was opposite the exit slit. The ratio:

$$\frac{\text{Photo-current caused by fluorescence of Anthracene}}{\text{Photo-current caused by fluorescence of Sodium Salicylate}}$$

was evaluated for a whole range of exciting wavelengths. (The wavelength of the radiation passing through the exit slit was obtained as described in Chapter IV). A photomultiplier tube is a device such that the photo-current which it yields is proportional to the number of quanta of given wavelengths falling on its photo-cathode, and therefore the ratios which were determined were measures of the quantum efficiencies of Anthracene relative to Sodium Salicylate for various exciting wavelengths.

The fluorescence excitation spectrum of Anthracene relative to Sodium Salicylate was obtained by plotting the ratio of the photo-currents against the wavelength of the exciting radiation. Sodium Salicylate has been found to have a fluorescence excitation spectrum which is almost independent of wavelength between 900 A and 3300 A (1.5, 3.3, 3.4), and therefore the relative excitation spectrum should be very similar to the absolute excitation spectrum of Anthracene, with the difference that the former spectrum has an arbitrary intensity scale.

The validity of the method described for the measurement of excitation spectra depends on the following factors:-

(1) None of the exciting radiation is transmitted by the fluorescent chemicals;

(2) The intensity of fluorescence is proportional to the intensity of the exciting radiation;

(3) The wavelengths of fluorescence spectra are independent of the wavelength of the exciting radiation (1.6).

EFFECTS OF THE REFLECTIVITY OF ANTHRACENE ON EXCITATION SPECTRA:

The percentage of monochromatic radiation reflected from the surface of an Anthracene crystal depends on the wavelength of the radiation. Measurements have shown that the spectral variations in the reflection coefficient of Anthracene crystals are of the order of 5%, and act to

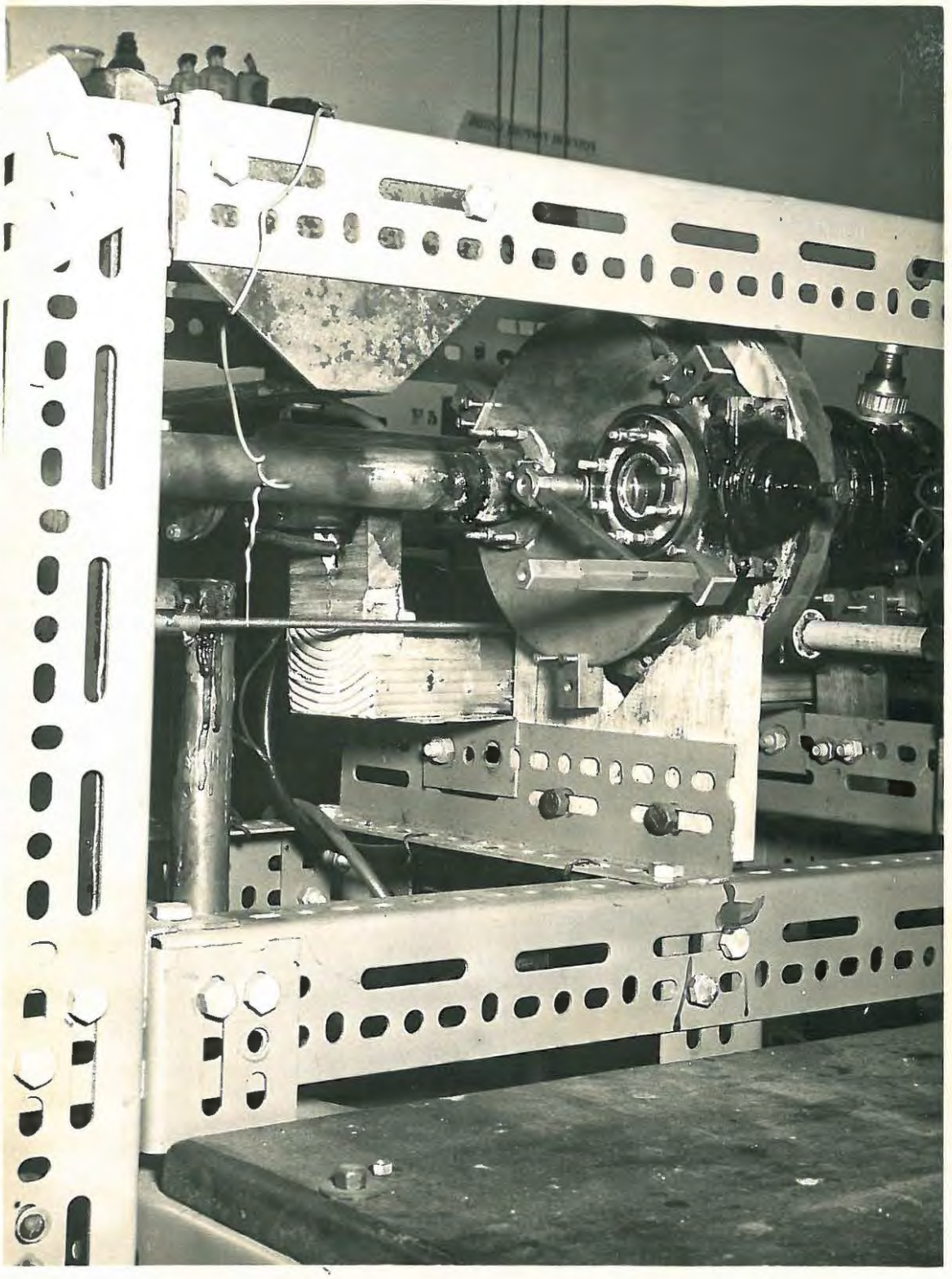

PLATE III: THE CRYSTAL CLEAVING DEVICE.

oppose variations in the excitation spectrum (1.4). The reflectivity spectrum of powdered Anthracene has been measured (3.6), and the wavelengths of maxima in the spectrum are given as 3750 A, 3535 A, 3375 A, 2830 A. The first three of these maxima coincide closely with the minima in the near ultra-violet excitation spectrum of crystalline Anthracene (1.4). If the reflectivity spectrum of powdered Anthracene has maxima at the same wavelengths as the reflectivity spectrum of the crystal, variations in the reflectivity coefficient with wavelength would tend to enhance the minima in the excitation spectrum of the crystal.

An attempt was made to measure the reflectivity spectrum of an Anthracene crystal between the wavelengths 2300 A and 3100 A with a Beckmann monochromator. No reproducible spectra were obtained, but it appeared from the measurements that the magnitude of the reflection coefficient was not greater than 8% at any wavelength between 2300 A and 3100 A. No corrections for variation in the reflectivity of Anthracene crystals with wavelength have been applied to the excitation spectra illustrated in this thesis.

SODIUM SALICYLATE LAYERS:

The excitation spectra of Sodium Salicylate layers of different thicknesses have been measured for exciting wavelengths between 2300 A and 3300 A (3.4). The intensity of the spectrum of a layer of Sodium Salicylate of surface density ·2 mg/sq. cm. was found to be almost independent of wavelength, while there was a maximum of intensity at about the wavelength 2700 A in the spectrum of a thicker layer of surface density 1.6 mg/sq.cm.

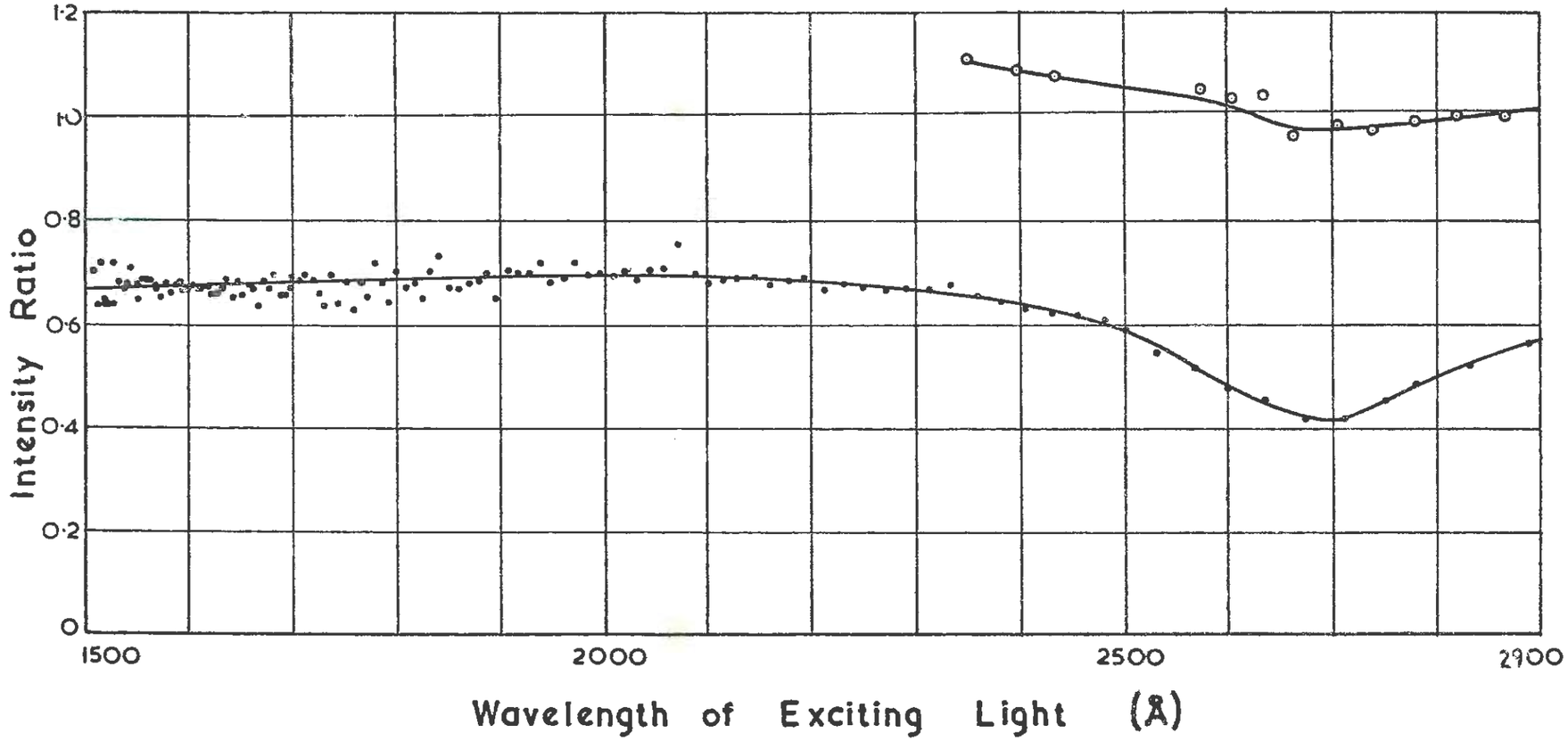
1·2
1·0
0·8
0·6
0·4
0·2
0
Intensity Ratio
1500
2000
2500
2900
Wavelength of Exciting Light (Å)

DIAGRAM 3.3

Two Sodium Salicylate layers having surface densities of ·2 mg/sq. cm. were prepared, each on faces of quartz discs, by evaporation of dilute solutions of Sodium Salicylate in distilled water from the discs. (A little difficulty was experienced before apparently uniform layers were obtained). The quartz discs were each glued over holes in the brass disc inside the chamber, and the excitation spectrum of the thin relative to the thicker layer was measured in the same way as the excitation spectrum of an Anthracene crystal relative to a Sodium Salicylate layer.

The ratio:

$$\frac{\text{Intensity of fluorescence of thin layer}}{\text{Intensity of fluorescence of thick layer}}$$ is shown in

Diagram 3.3 as a function of the wavelength of the exciting light. There is a minimum in this spectrum at the wavelength 2700 A which corresponds to the maximum which was observed in the spectrum of the thicker layer. The excitation spectra of Anthracene crystals were measured relative to a thin layer of Sodium Salicylate, for it is likely that the absolute excitation spectrum of a thin layer does not have a maximum near the wavelength 2700 A.

## IDENTIFICATION OF THE CRYSTALLOGRAPHIC PLANES OF ANTHRACENE:

The Anthracene crystals were mounted in the holes in the brass disc inside the cleaving chamber in such a way that when a particular crystal was opposite the exit slit, the exciting radiation, impinged almost normally on a face of the crystal. The Anthracene molecule is planar, and its structure is illustrated in Diagram 3.4. It proved desirable to know the angle between the normals to the planes of the molecules in the lattice and the normals to

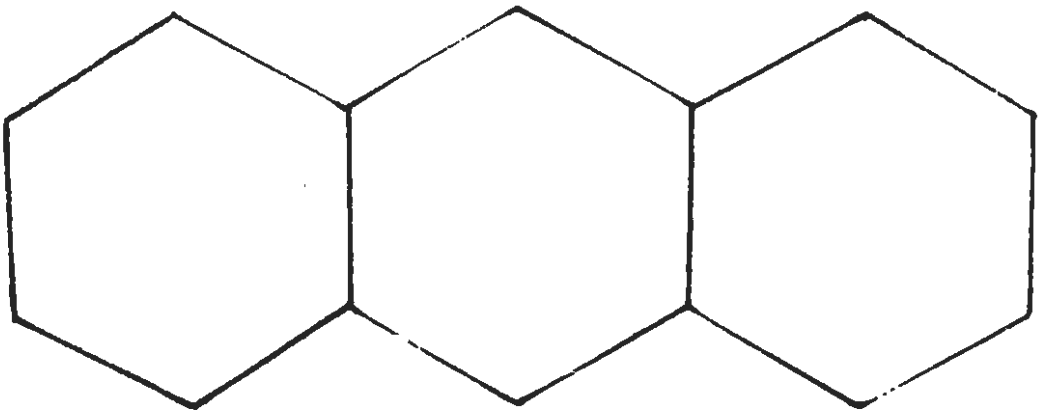

THE ANTHRACENE MOLECULE

DIAGRAM 3.4

the faces of the Anthracene crystals (which were in the shape of centimeter cubes), so that the orientation of the molecules with respect to the direction of the exciting light would be known.

The crystal of Anthracene, which is monoclinic, cleaves "perfectly" in the (001) crystallographic plane (3.7). (The planes are described in terms of the Miller indices). The surfaces of one pair of opposite faces of the Anthracene cubes appeared very smooth and shiny, and the crystals cleaved easily in planes parallel to these faces, which planes were presumed to be the (001) planes. (The two faces of a crystal parallel to the (001) crystallographic planes will be described as the (001) faces of the crystal, and fluorescence excitation spectra measured when the exciting light fell on either of these faces will be described as the (001) spectra). A study made at the Rhodes University Geology Department, suggested that there were lines of cleavage in a particular crystal perpendicular to the (001) faces. Anthracene crystals cleave distinctly in the (010) crystallographic planes which are perpendicular to the (001) planes (3.7).

When a monochromatic ray of light falls on a birefringent crystal such as Anthracene, there are in general, two refracted rays which are polarised at right angles to each other. There will be two directions in the crystal along which components of the two rays will be transmitted with the same velocity, and these directions are called the optic axes. The optic plane is the plane (or set of planes) in the crystal parallel to both optic axes, and the (010) plane of an Anthracene crystal coincides with the optic plane (3.7).

DIAGRAM 3.5

A single ray of light incident in a certain direction on a doubly refracting crystal such as Anthracene will give rise to a cone of rays inside the crystal, and the optic plane passes through the centres of the circular sections of the cone (3.8). If the angle between an edge of the face of an Anthracene cube parallel to the (001) crystallographic planes and the projection of this line on the (001) planes could be determined, the direction of the (010) planes in the cube would be known.

One side of an Anthracene cube was glued to a flat piece of metal foil so that a side of the cube was directly over a pinhole in the foil. Sodium light from a small hole in a screen about twenty centimeters from the cube was allowed to pass through the pinhole, and two images of the pinhole could be seen in the crystal from the opposite side of the crystal to the foil. The orientation of the crystal with respect to the direction between the small hole in the screen and the pinhole in the foil was varied until the two images of the pinhole came together and formed a ring of light on the surface of the crystal. The photograph of such a ring is given in Diagram 3.5. The ring is not clearly defined, probably because of cracks inside the crystal, and the rough condition of the surfaces. The ring appeared better to the eye than it appears in the photograph.

Two marks were made on the surface of the crystal, one where the pinhole in the foil was situated, the other where the centre of the ring of light on the other side of the crystal was estimated to be. The straight line joining the two marks on the surface would be expected to lie in the optic plane of the crystal. As it was found that the two marks were nearly

the same distance from one of the faces of the cube perpendicular to the (001) faces, it was concluded that a pair of opposite faces of the cube were nearly parallel to the optic (010) plane. Planes perpendicular to both the (010) and (001) planes will be described as (1'00) planes, and it will be assumed that the orthogonal planes were actually parallel to the faces of the particular Anthracene cube.

If orthogonal axes x,y,z' are chosen in the Anthracene lattice so that the x,y,z' axes lie in the (001), (010) and (1'00) planes respectively, the equation of the plane which is parallel to the planes of the molecules is given by:

$$x - .533y + .500z' = 0 \quad (3.9).$$

It may be shown from this equation that the normals to the planes of the molecules make angles of 24°, 25.5° and 54° with the (001), (010) and (1'00) crystallographic planes.

THE HYDROGEN SPECTRUM:

The spectrograph was prepared for the measurement of spectra, as has been described, and the brass disc inside the cleaving chamber was rotated so that the Sodium Salicylate layer was opposite the exit slit. The photo-current resulting from the fluorescence of the Sodium Salicylate was plotted as a function of the wavelength of the radiation passing through the exit slit, and in this way a Hydrogen spectrum was obtained. (The method of obtaining the wavelength of the radiation passing through the exit

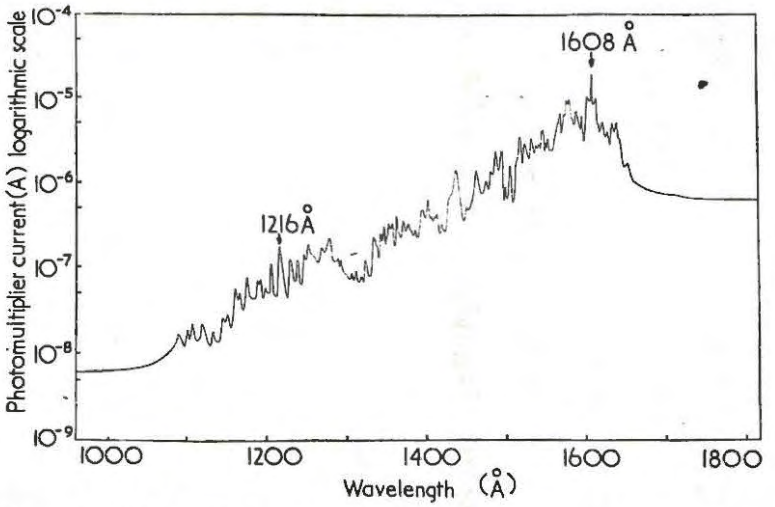


Fig. 7. Plot of spectrum of hydrogen positive-column discharge

DIAGRAM 3.7

slit will be described in Chapter IV). A typical Hydrogen spectrum is illustrated in Diagram 3.6. A Hydrogen spectrum measured with a grating spectrograph is shown for comparison in Diagram 3.7. (3.5)

The wavelength of the very intense maximum in the Hydrogen spectrum is known to be 1608.2 A (3.5, 3.10). The wavelengths of some of the maxima in Diagram 3.6 were estimated to be 1712.6 A, 1730.5 A, 1751 A, 1779 A, 1793 A and 1808 A. Wavelengths which correspond to these wavelengths were estimated from a photograph of a Hydrogen spectrum to be 1712 A, 1730 A, 1748 A (faint), 1773 A, 1792 A, 1811 A (3.10).

The intensity of the Hydrogen spectrum becomes weak at wavelengths below 1500 A, probably because the reflectivity of Aluminium becomes low at these wavelengths (2.1). A few Hydrogen spectrum lines of low intensity were observed between the wavelengths 1350 A and 1500 A.

EFFECTS OF SCATTERED LIGHT ON SPECTRA:

When the spectrograph was in operation, a certain amount of scattered light passed through the exit slit together with the ultra-violet radiation from the discharge tube. It was explained in Chapter II that the intensity of scattered light changed very gradually as the wavelength of the ultra-violet radiation passing through the exit slit was varied. The scattered light would, therefore, not cause any spurous maxima or minima to appear in the Hydrogen spectrum in Diagram 3.6.

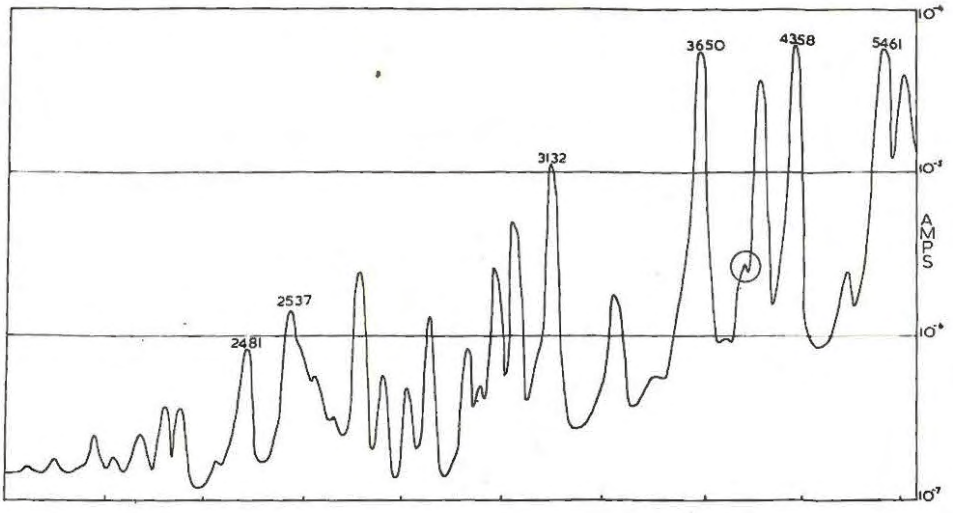


MERCURY CALIBRATION SPECTRUM. Counter reading plotted against photo-current.

DIAGRAM 4.1

It was not possible to obtain a reliable estimate of the percentage of scattered light in the ultra-violet radiation of any wavelength passing through the exit slit. The photo-currents corresponding to the weakest intensities in the Hydrogen spectrum in Diagram 3.6, were only three to four times greater than the maximum value of the photo-current corresponding to the scattered light measured as described in Chapter II.

It is therefore possible that the excitation spectra of Anthracene which were measured could be slightly distorted at the wavelengths where exciting radiation was weakest, for the intensity of an excitation spectrum at any wavelength was determined by the ratio of photo-currents, each of which would have been increased slightly by the presence of scattered light in the exciting radiation.

# DIAGRAM 3.6

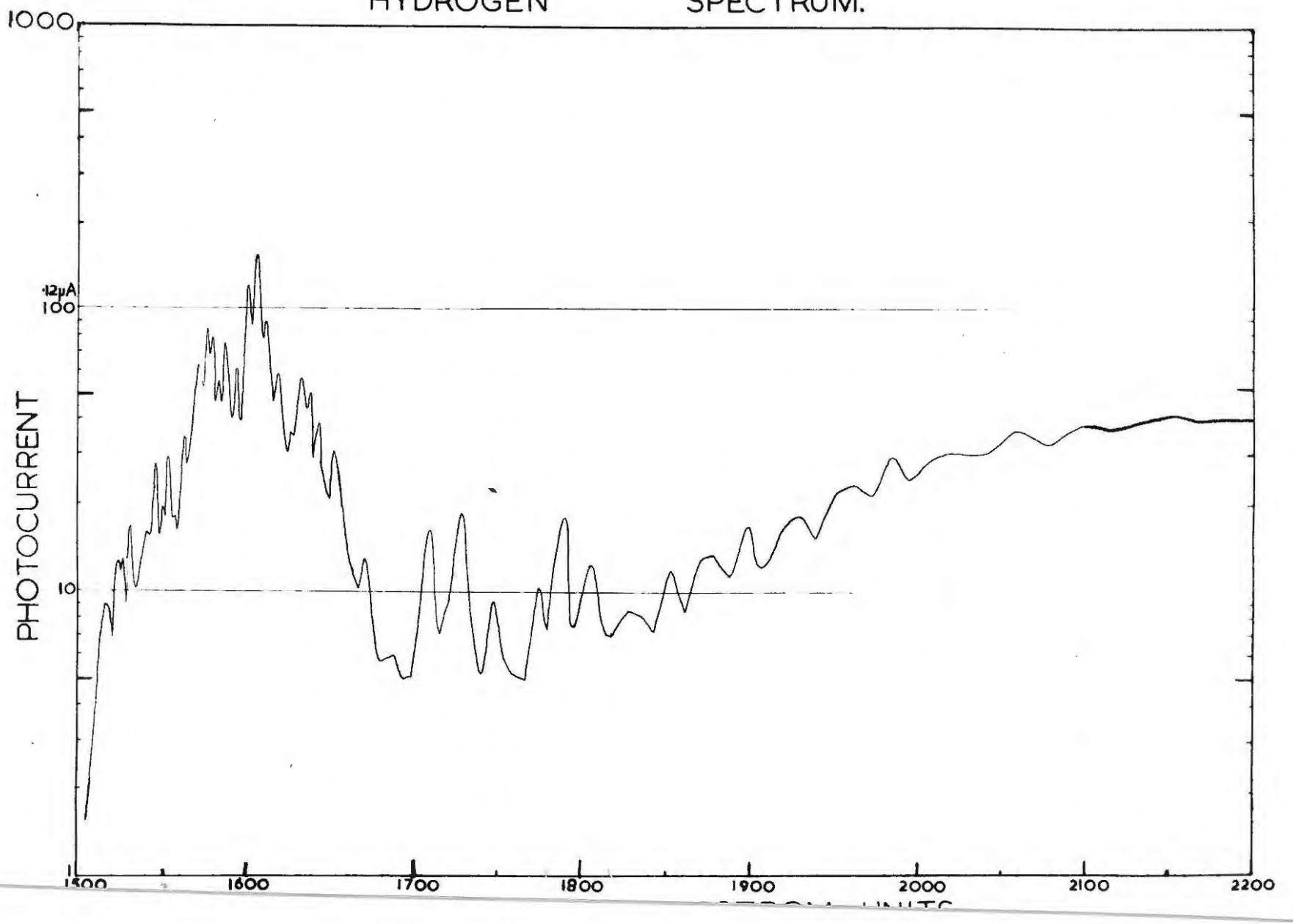
HYDROGEN SPECTRUM.
1000
·12μA
100
10
1
PHOTOCURRENT
1500
1600
1700
1800
1900
2000
2100
2200

TABLE II.

| λ (Å) | μ −1 | Nobs | Ncalc | Nobs-Ncalc. |
|---|---|---|---|---|
| 5461 | ·43537 | 312·78 | 313·11 | − ·33 |
| 4916 | ·43730 | 310·93 | 311·24 | − ·31 |
| 4358 | ·43996 | 308·35 | 308·65 | − ·30 |
| 4078 | ·44171 | 306·65 | 306·95 | − ·30 |
| 3650 | ·44544 | 303·63 | 303·31 | + ·32 |
| 3341·5 | ·44902 | 299·90 | 299·83 | + ·07 |
| 3132 | ·45220 | 296·45 | 296·74 | − ·29 |
| 3022 | ·45412 | 294·70 | 294·86 | − ·16 |
| 2955 | ·45548 | 293·64 | 293·55 | + ·09 |
| 2894 | ·45678 | 292·05 | 292·28 | − ·23 |
| 2815 | ·45858 | 290·20 | 290·53 | − ·33 |
| 2753 | ·46012 | 289·00 | 289·03 | − ·03 |
| 2699 | ·46152 | 287·80 | 287·67 | + ·13 |
| 2654 | ·46281 | 286·66 | 286·41 | + ·25 |
| 2537 | ·46657 | 283·05 | 282·75 | + ·30 |
| 2481 | ·46863 | 281·00 | 280·75 | + ·25 |
| 2399 | ·47194 | 277·52 | 277·52 | ·00 |
| 2378 | ·47283 | 276·68 | 276·66 | + ·02 |
| 2345 | ·47432 | 275·30 | 275·21 | + ·09 |
| 2325 | ·47524 | 274·05 | 274·31 | − ·26 |
| 2302 | ·47634 | 273·10 | 273·24 | − ·14 |
| 2253 | ·47887 | 271·00 | 270·78 | + ·22 |
| 2225 | ·48039 | 269·60 | 369·30 | + ·30 |
| 2002 | ·49599 | 254·25 | 254·12 | + ·13 |
| 1973 | ·49843 | 251·90 | 251·74 | + ·16 |
| 1942 | ·50140 | 249·10 | 248·85 | + ·25 |

# CHAPTER IV.

## THE CALIBRATION

### THE MERCURY SPECTRUM

An ultra-violet quartz Mercury lamp was placed opposite the entrance slit of the spectrograph, and a graph of the Mercury spectrum was obtained in the same way as the graph of the Hydrogen spectrum was obtained (Chapter III). The intensity of the Mercury spectrum at the exit slit is shown in Diagram 4.1 as a function of the counter reading N which measured the rotation of the rotary transmission shaft.

The wavelengths of the more intense lines of the Mercury spectrum were selected from tables (4.1) and were related to the more intense spectrum lines of Diagram 4.1. The spectrum of the Mercury lamp was photographed using a small grating spectrograph, and a comparison of the photograph with Diagram 4.1 enabled most of the lines of wavelength longer than 2400A to be identified. The wavelengths of the identified spectrum lines were plotted against the corresponding readings of the counter N, and the first section of the calibration graph was obtained.

The wavelengths of the Mercury lines are listed in Table II together with the corresponding counter readings.

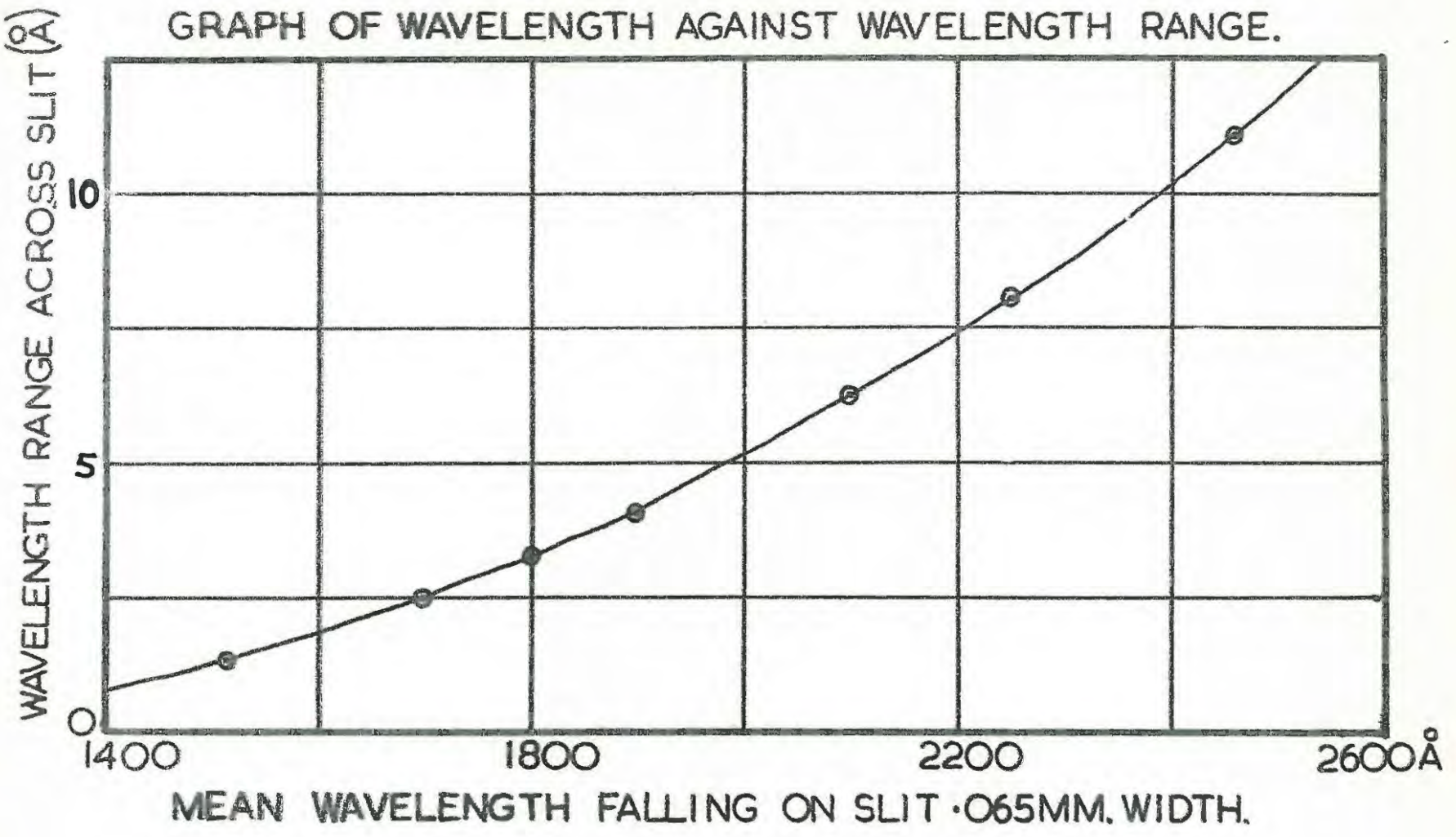
GRAPH OF WAVELENGTH AGAINST WAVELENGTH RANGE.
WAVELENGTH RANGE ACROSS SLIT (Å)
10
5
0
1400
1800
2200
2600Å
MEAN WAVELENGTH FALLING ON SLIT ·065MM. WIDTH.

DIAGRAM 4.2

The wavelengths of two Mercury spectrum lines which were not listed in any of the tables consulted are given as 1923±7A and 1902±7A.

The range of wavelengths passing through the exit slit was always finite. Diagram 4.2 shows how the range of wavelengths depended on the mean wavelength passing through the exit slit. This graph was useful when deciding whether or not Mercury spectrum lines of Diagram 4.1 were the resultant of a combination of two or more lines. As the wavelengths of such spectrum lines would be uncertain, they were not used for calibration purposes.

EXTENSION OF THE CALIBRATION CURVE

Let $\mu$ and $\mu_o$ be the refractive indices of Calcium Fluoride for wavelengths $\lambda$ and $\lambda_o$.

Consider a ray of wavelength $\lambda$ which is incident at a small angle on a refracting face of the thin Calcium Fluoride prism in a plane perpendicular to its refracting edge. If the ray passes through the prism, it will be deviated through an angle $(\mu-1)A$ where A is the refracting angle of the prism. If the ray is reflected back again through the prism, the total angle of deviation it will undergo as a result of refraction by the prism will be given by

$$D = 2(\mu-1)A \qquad \ldots\ldots\ldots\ldots (1)$$

The total deviation of a ray of wavelength $\lambda_o$ will be given by:

$$D_o = 2(\mu_o - 1)A \qquad \ldots\ldots\ldots(2)$$

If (1) and (2) are subtracted, it follows that:

$$D - D_o = 2(\mu - \mu_o)A \qquad \ldots\ldots\ldots(3)$$

Let N and $N_o$ be the readings on the counter when wavelengths $\lambda$ and $\lambda_o$ pass through the exit slit of the spectrograph. The mechanism by means of which the prism table was rotated was such that the rotation of the rotary transmission shaft was proportional to the rotation of the table. The angle $D - D_o$ through which the prism would have to rotate in order for the wavelength at the exit slit to change from $\lambda$ to $\lambda_o$ is therefore proportional to $N - N_o$.

It follows that:

$$2(\mu - \mu_o)A = K(N-N_o) \qquad \ldots\ldots\ldots(4)$$

where K is a constant.

If $N_o$ (and therefore $\mu_o$ and $\lambda_o$) are taken to be constant, it follows from equation (4) that:

$$(\mu - 1) = \frac{K}{2A} N - \left[\frac{KN_o}{2A} - \mu_o + 1\right] \ldots\ldots(5)$$

$$\text{or } \mu - 1 = BN + C \qquad \ldots\ldots(6)$$

where B and C are constants, the values of which may be determined by comparing (5) and (6).

Values of the refractive indices of Calcium Fluoride for various wavelengths are listed in tables (2.2).

A large graph of refractive index against wavelength was drawn, and the refractive indices for each of the Mercury wavelengths listed in Table II were estimated from it. These refractive indices and the corresponding counter readings for the Mercury lines were substituted in (6), and a number of linear equations in B and C were obtained. These equations were solved and the mean values of B and C were found.

Equation (6) was used to calculate the counter reading N corresponding to any wavelength for which the refractive index was known. The refractive indices for many wavelengths in the vacuum ultra-violet are known (2.2), and it was therefore possible to extend the calibration graph from longer wavelengths to 1311A.

The Hydrogen spectrum is known to have a maximum of intensity in the middle vacuum ultra-violet at the wavelength 1608A (3.5, 3.10). The maximum of intensity was observed with the spectrograph, and the corresponding wavelength was established from the calibration graph (obtained as described) to be 1605A. The constants B and C of equation (6) were therefore recalculated in the following manner, so that a new calibration graph was obtained from which the wavelength of the maximum of intensity would be estimated as 1608A. One linear equation was obtained by a summation of the linear equations in B and C obtained as described.

Another was obtained by substituting in (6) the

refractive index for the wavelength 1608A, and the counter reading corresponding to the maximum of intensity.

These two equations were solved for B and C. The new calibration graph was then made as before using equation (6) and the new values of B and C. The graph which was used for finding the wavelengths at the exit slit corresponding to the counter readings was obtained from the formula :

$$\mu - 1 = -1{\cdot}02744 \times 10^{-3} N + {\cdot}75708 \quad \ldots\ldots\ldots \quad (8)$$

ACCURACY OF THE CALIBRATION

One of the weak points of the spectrograph was the lack of sufficient rigidity in its structure. The calibration was altered by the mechanical stresses brought about by bolting the steel pipe which formed the main vacuum chamber to the steel base plate. As the counter readings corresponding to the wavelengths of given spectrum lines at the exit slit changed by as much as .6 of a turn, the spectrograph had to be recalibrated if the steel pipe was bolted. The stresses brought about by evacuating the spectrograph changed the counter readings by about one tenth of a turn.

Spectrum lines were reproducible at the exit slit usually to within .2 of a turn of the counter on a given day. The reproducibility was limited by imperfections of the mechanism by means of which the prism table was rotated. Sometimes

TABLE III.

| $\lambda$(A) | 3000 | 2500 | 2000 | 1600 | 1500 |
|---|---|---|---|---|---|
| $\Delta\lambda(\pm$A) | 25 | 13 | 6 | 2·2 | 1·6 |

when the spectrograph was used on subsequent days, the counter readings of spectrum lines had changed by as much as ·4 of a turn from their original values. These changes may be attributed to temperature changes affecting the mechanical structure of the spectrograph.

When the wavelengths of spectrum lines at the exit slit were measured from the calibration graph, it was assumed that the error in the counter reading would not exceed $\pm$·5 of a turn. The corresponding wavelength errors which might be expected at various wavelengths are given in Table III.

DIRECT CALIBRATION OF THE SPECTROGRAPH AT SHORTER WAVELENGTHS

An attempt was made to calibrate the counter in terms of wavelengths of known spectrum lines in the vacuum ultra-violet region. A Schüler hollow cathode discharge tube was constructed for the purpose of exciting the spectrum lines.

A Schüler tube has two electrodes, an anode and a cathode which has a cavity in it. Spectrum lines of the material of the cathode or of a substance placed in the cavity may be excited in an atmosphere of an inert gas by means of a direct-current discharge between the electrodes. The Schüler tube constructed was a modification of one which has been described (4.2), and its cross-section is illustrated in Diagram 4.3.

The electrodes were made of commercial Aluminium, and

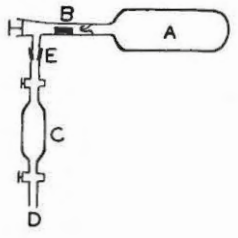


A ARGON BOTTLE.
B METAL CYLINDER.
C SMALL RESEVOIR.
D TO SCHULER TUBE.
E GROUNDGLASS JOINT.

DIAGRAM 4.4

consisted of a hollow cylindrical anode B, and a cylindrical cathode A. The end of the cathode facing the anode was tapered slightly in order to concentrate the discharge from the anode into the cylindrical cavity in the cathode. The tube was connected to the spectrograph by means of the flange G. The cathode was waxed into the farther end of the tube from the spectrograph so that it was separated by about one centimeter from the anode, and it was water-cooled in order that the heat of the discharge should not melt the wax seal. Radiation excited by the discharge in the cylindrical cavity of the cathode passed through the hollow anode and the length of the tube to the entrance slit of the spectrograph.

Spectrally pure Argon was introduced into the Schüler tube through the inlet E (Diagram 4.3). The Argon was contained in a glass bottle A which was closed by means of a delicate glass seal inside the neck. (Diagram 4.4). A small evacuated reservoir C was filled with Argon from the bottle. Argon was allowed to leak from the small reservoir through tube D to fill the whole spectrograph and the Schüler tube to a pressure of a few millimeters of Mercury.

When a positive stabilised voltage was applied at the anode, a discharge to the earthed cathode was observed. A resistance was placed in series with the discharge in order to limit the current to 150 milliamps. The voltage at the anode

# DIAGRAM 4.3

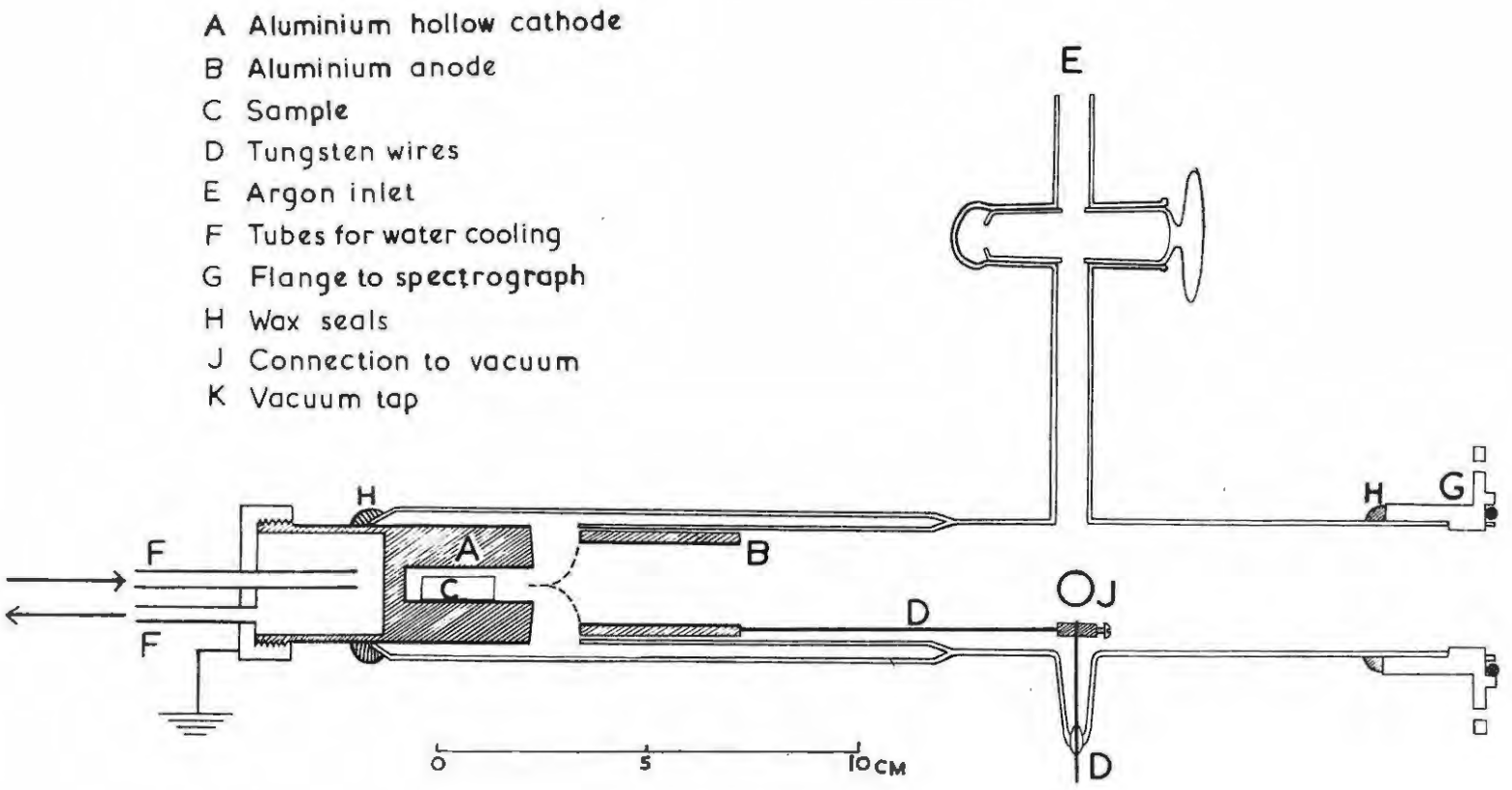


HOLLOW CATHODE SCHULER DISCHARGE TUBE

TABLE IV.

ZINC SPECTRUM LINES

| Counter Reading | Estimated Wavelength (A) | Relative Intensity | Nearest Wavelength from Tables (A) | Intensity |
|---|---|---|---|---|
| 264•3 | 2141 ± 7 | 170 | 2138•6 (4.1) | 800 |
| 257•5 | 2056 ± 6 | 3 | 2061•9 (4.1) | 100 |
| 255•8 | 2022 ± 6 | 6 | 2025•5 (4.1) | 200 |
| 225•1 | 1744 ± 3 | 1 | 1743•6 (4.1) | 10 |
| 210•2 | 1658 ± 3 | 6 | ? | - |
| 205•3 | 1634 ± 2 | 3 | 1632•1 (3.6) | 4 |
| 195•1 | 1588 ± 2 | 3 | 1589•6 (3.6) | 10 |
| 188•3 | 1562 ± 2 | 6 | ? | - |

was between 500V and 700V.

Some scraps of very pure copper were placed in the cavity in the cathode, and the radiation excited in the cavity by the discharge was studied with the spectrograph. No spectrum lines of wavelength shorter than 2100A were observed, probably because the copper did not acquire a high enough temperature (4.3). The intensity of the radiation was found to be a maximum when the Argon pressure in the tube was about 1 mm. Hg. If the pressure was reduced much below 1 mm. Hg., a pale steel-blue discharge from the anode to the flange G (Diagram 4.3) commenced.

A new pair of electrodes were made for the Schüler tube so that there should be no traces of the copper on them. A sample of very pure Zinc was placed in the cavity of the new cathode, and the radiation excited by the discharge was studied as before. The estimated wavelengths and relative intensities of spectrum lines which were excited in the vacuum ultra-violet region are listed in Table IV. The nearest wave-lengths to these in tables of Zinc spectrum lines are also given in Table IV. Two of the observed spectrum lines could not be identified as Zinc lines. As there was some doubt about the identification of the remaining lines, they were not used for calibration purposes.

FLUORESCENCE EXCITATION SPECTRA OF ANTHRACENE.

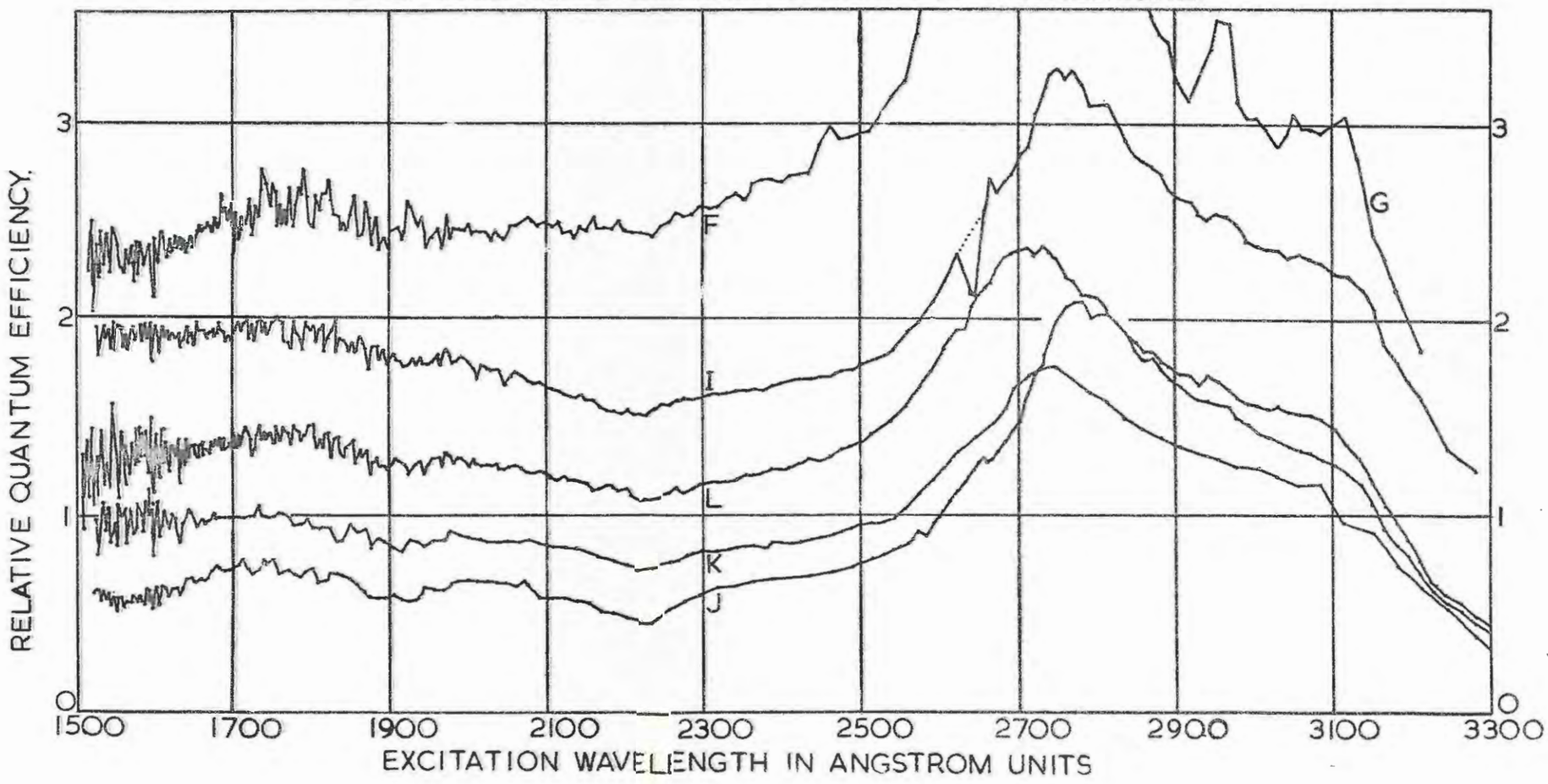


DIAGRAM 5.1

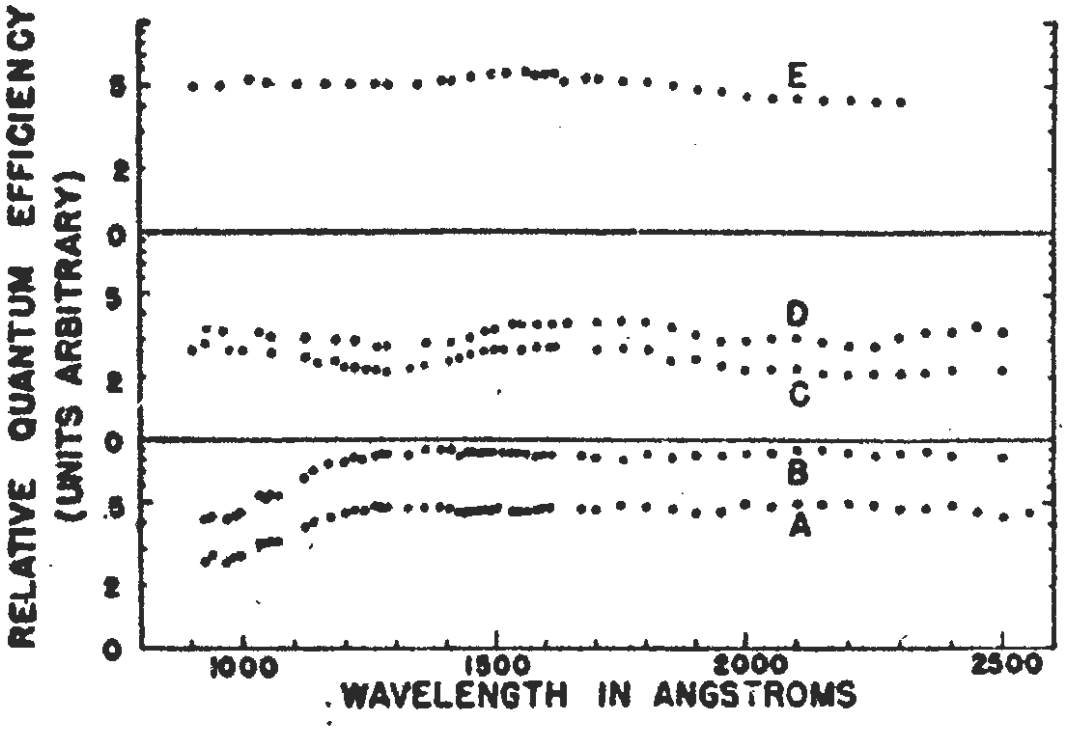


FIG. 6. Relative quantum efficiencies of fluorescence: A and B, Cenco pump oil using different 1P21 photomultipliers; C and D, two anthracene crystals; E, sodium salicylate.

DIAGRAM 5.2

# CHAPTER V.

## RESULTS AND DISCUSSION.

### MINIMA IN EXCITATION SPECTRA:

Some relative fluorescence excitation spectra of an Anthracene crystal were measured as described in Chapter III, and are illustrated in Diagram 5.1. The wavelengths of two minima in the spectra were estimated to be 2220 ± 12 A, and 1910 ± 10 A. These minima also appear in the spectra in Diagram 5.2, which were measured by other workers (1.5). Two maxima have been measured in the absorption spectrum of crystalline Anthracene at wavelengths slightly shorter than the minima in the excitation spectrum, namely at 1890 A and 2200 A (5.1). Other workers have found that maxima in the absorption spectrum occur at slightly shorter wavelengths than minima in the excitation spectrum of crystalline Anthracene in the near ultra-violet region (1.4).

### THE EFFECTS OF POLISHING:

The surfaces of the Anthracene crystals appeared to have been polished by the manufacturers of the crystals. An excitation spectrum measured when the exciting light fell on a polished surface of a crystal will be referred to as the excitation spectrum of a polished crystal. If the exciting light fell on an unpolished surface, the excitation spectrum will be described as that of a cleaved crystal.

DIAGRAM 5.3

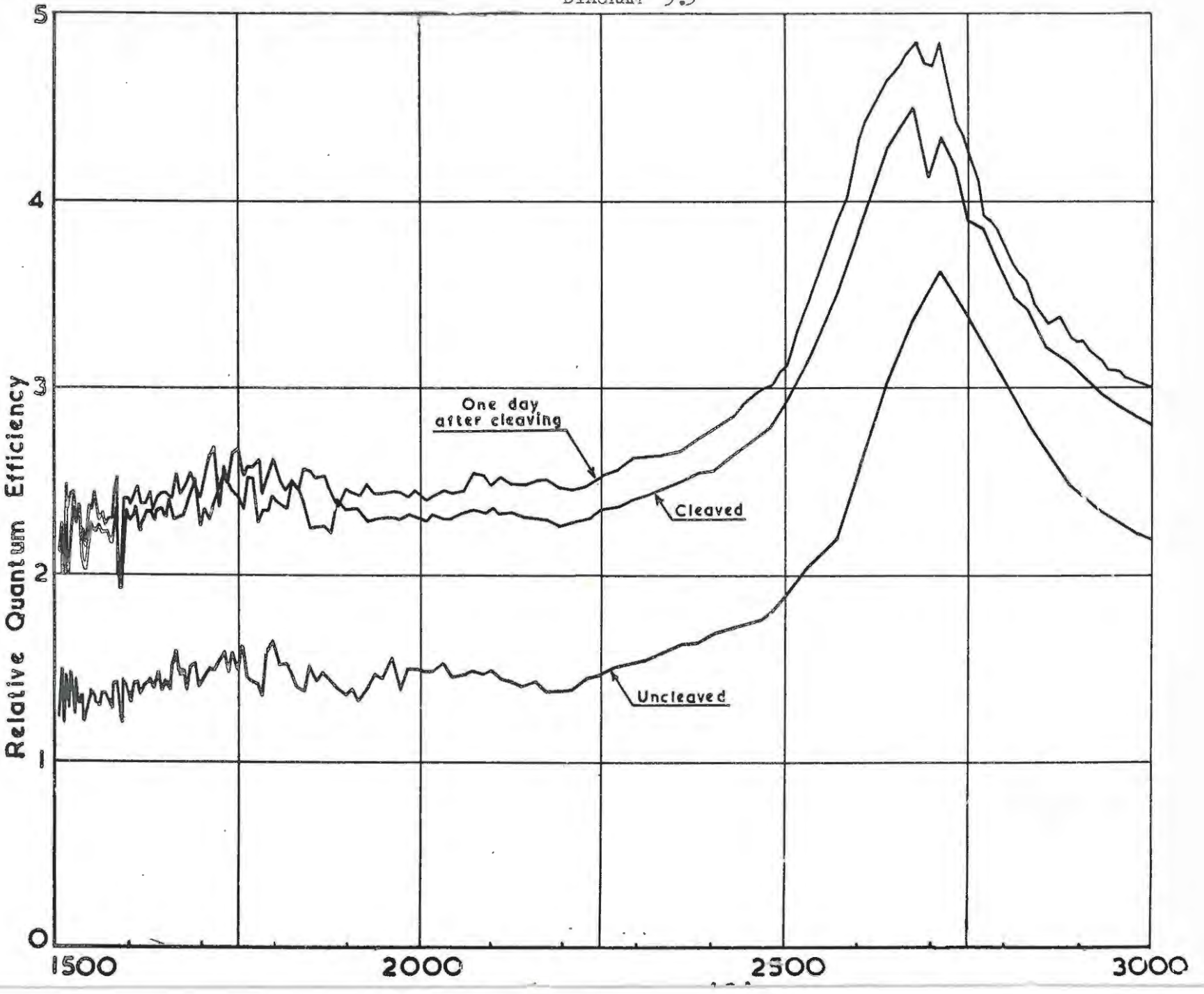
Relative Quantum Efficiency
5
4
3
2
1
0
1500
2000
2500
3000
One day after cleaving
Cleaved
Uncleaved

The excitation spectra of polished and cleaved crystals were similar, but certain differences between them were observed. The excitation spectra of polished crystals were less intense than those of cleaved crystals, in accordance with the results of other workers (5.2). The minima at the wavelengths 1910 A and 2220 A in the excitation spectra of polished crystals appeared rather deeper than the corresponding minima in the excitation spectra of cleaved crystals. Also, an intense maximum at the wavelength 2710 ± 20 A in the excitation spectra of cleaved crystals occurred at a slightly shorter wavelength than the corresponding maximum in the excitation spectra of polished crystals. These differences are illustrated by the (001) spectra in Diagram 5.3, and the (1'00) spectra J, K and L in Diagram 5.1. The least intense spectra in each of Diagrams 5.1 and 5.3 are spectra of polished crystals, and all the other spectra in these diagrams are those of cleaved crystals.

The intensity of fluorescence from a polished crystal excited by a band of ultra-violet light of constant intensity has been found to decrease slowly within a few days to about one third of the intensity measured soon after the crystal was polished. If the crystal was cleaved in air so that the ultra-violet light could fall on an unpolished surface, the intensity remained constant even if the crystal was stored for a few days in air or in oxygen at 100°C. It was suggested that the polishing caused an increased reaction rate of the surface molecules of the crystal with oxygen, and that as the surface became oxidised, the intensity of fluorescence decreased (5.2). It is possible that the excitation spectra of polished Anthracene

crystals are characteristic of an oxide on the surface rather than of the substance beneath the surface.

Anthraquinone, an oxide of Anthracene, is not fluorescent in the solid state. The oxide on the surface could be Anthraquinone, for thin adsorbed layers of Anthraquinone are known to be fluorescent (5.3). Dianthracene, a polymer of Anthracene, may be formed photochemically on the surfaces of the crystals by ultra-violet irradiation (5.4). Dianthracene has different crystalline structure and physical properties from Anthracene, but its fluorescence spectrum is identical to that of Anthracene (5.5).

THE EFFECTS OF CLEAVAGE:

The intensities of fluorescence excitation spectra of polished crystals were found to have increased at all wavelengths if the spectra were remeasured after cleavage of the crystals in a vacuum as described in Chapter III. It was also found that the intensities of the spectra went on increasing and reached a maximum within twenty-four hours after the cleavage.

The effects described are illustrated in Diagrams 5.1 and 5.3. The least intense curves in each of these diagrams represent the fluorescence excitation spectra of polished crystals. The curves next above the least intense curves illustrate the increase in intensity of the spectra after cleavage of the crystals in a vacuum . Curve L in Diagram 5.1 and the topmost curve ir Diagram 5.3 illustrate the further increase in intensity of the spectra within twenty-four hours. The intensity of spectrum K

at all wavelengths increased within five hours by at least fifty per cent of the difference in intensity between spectra K and L at the wavelength 2500 A. The increase was occurring while the crystal was inside the vacuum in the spectrograph.

The spectrograph was filled with air so that the effects on the intensities of the excitation spectra of storage in air of the cleaved crystals could be studied. It was found that storage of the crystals in air for periods of up to three weeks did not affect by any measurable amount the intensities of the excitation spectra which had already reached a maximum after cleavage of the crystals.

The slow increase to a maximum value of the intensity of the excitation spectrum of a crystal which has been cleaved in a vacuum might be caused by a gradual combination of the oxygen in the residual air in the vacuum with molecules on the surface of the crystal. (There is evidence that oxygen combines with the surface molecules of Anthracene crystals to form an oxide or peroxide of Anthracene (5.6)). Such a conclusion would be surprising, for oxygen quenches the fluorescence of solutions of Anthracene (1.9). Nitrogen has no effect on the intensity of fluorescence of Anthracene solutions (5.7), and probably does not affect the intensity of fluorescence of crystals. It is possible that pure Anthracene is non-fluorescent, and that Anthracene crystals fluoresce by virtue of traces of oxygen impurity combined with some of the molecules in the lattice.

The slow increase in intensity might be caused by a gradual self-annealing of the newly formed surface of the crystal. (Dr. J.A. Gledhill and the writer are indebted to Dr. D.B. Holt of the University of the Witwatersrand for this suggestion given in a discussion following a paper read at a conference of the S.A. Institute of Physics, Stellenbosch, July 1959). Evidence has been obtained recently to suggest that Anthracene crystals might fluoresce by virtue of strains and imperfections in the lattice (5.8). The slow increase in intensity might also be the result of a gradual condensation of water vapour in the vacuum on the surface of the crystal on which the exciting radiation falls. Inclusion of a small quantity of drying agent in the main vacuum chamber of the spectrograph did not prevent the slow increase. A study of changes in the intensity of the excitation spectrum of a crystal which has been cleaved in an atmosphere of a pure dry rare gas might establish whether or not the slow increase in intensity of cleaved crystals is caused by oxygen.

CHANGES IN THE EXCITATION SPECTRA OF CLEAVED CRYSTALS:

It has been explained that the intensities of the excitation spectra of cleaved crystals attain a maximum, and that the intensities do not decrease again if the crystals are stored in air. When some measurements of the excitation spectra of cleaved crystals were made within a few days of each other (and the crystals were stored in air at atmospheric pressure in the intervals between the measurements), it was found that maxima of intensity had begun to "grow" on the spectra between the wavelengths 2300 A and 3300 A.

DIAGRAM 5.4

EXCITATION SPECTRA SHOWING RELATIVE POSITIONS OF PEAK.

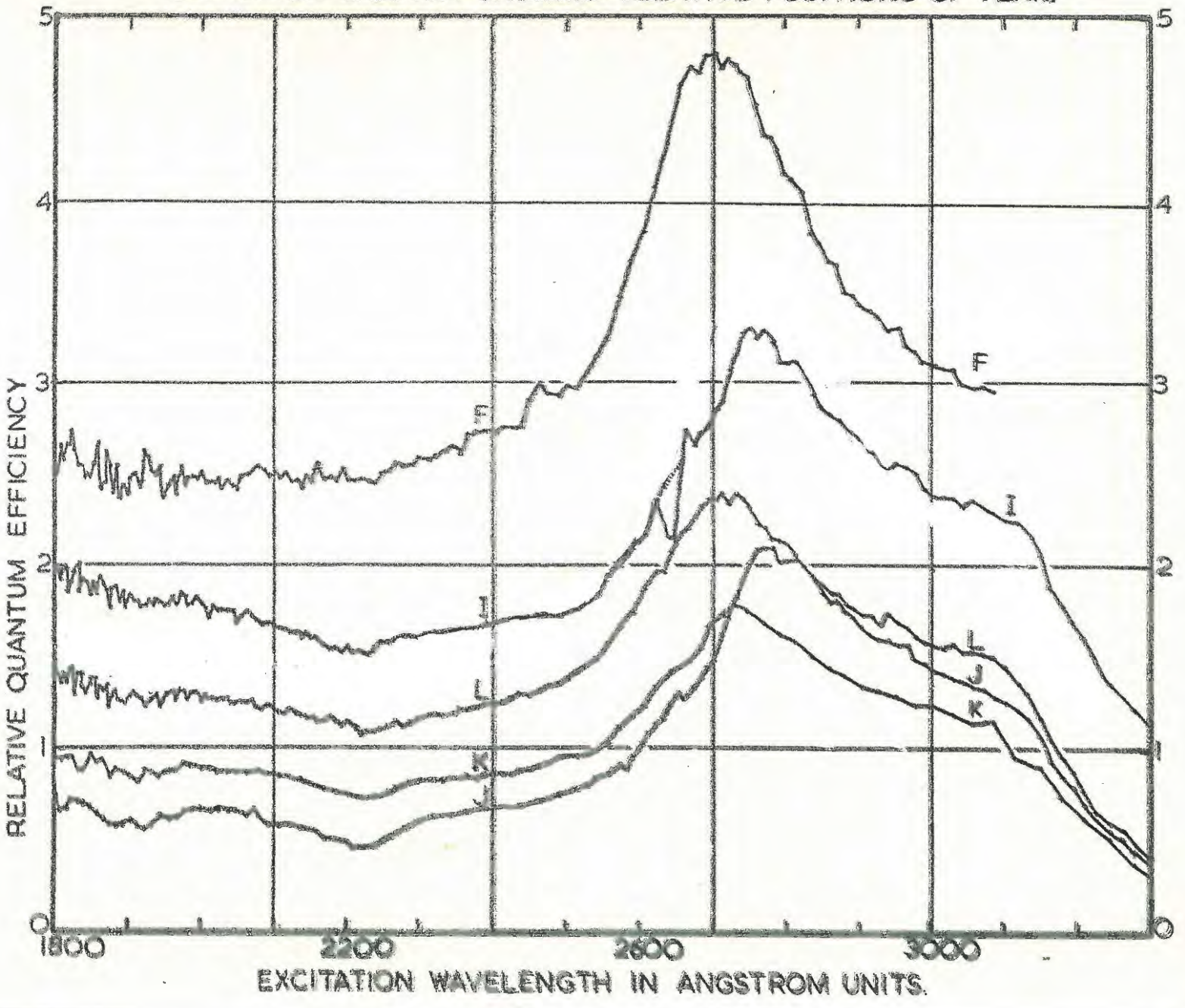

Some of these maxima appear weakly in the excitation spectrum J of a polished crystal in Diagram 5.4. When the excitation spectrum was remeasured soon after cleavage of the crystal in a vacuum, all trace of the maxima had disappeared (Curve K). When the spectrum was measured again, six days later, evidence of the maxima had reappeared (Curve L). The maxima hardly appear in the (001) excitation spectra illustrated in Diagram 5.3. Curve F in Diagram 5.4 illustrates a remeasurement of the spectrum of maximum intensity in Diagram 5.3 made after the crystal had been exposed to laboratory air for six days. A comparison of these two curves shows that a maximum has appeared in curve F at about the wavelength 2470 A. The measurement of curve F was repeated after a further three weeks exposure of the crystal to laboratory air, and curve G in Diagram 5.1 was obtained.(It was not possible to obtain the whole of curve G, for the spectrograph failed to function satisfactorily before the measurement was completed). The maxima have become very strong in curve G.

The estimated wavelengths of some of these maxima are listed in Table V, together with wavelengths of maxima in the "photo-conductivity spectrum" of Anthracene (5.9). It would appear that the wavelengths of three of the maxima in the photo-conductivity spectrum (3140 A, 3060 A, 2960 A) correspond to the wavelengths of three of the maxima which have "grown" in the excitation spectrum. The photo-conductivity spectrum has been shown to have maxima at the same wavelength as many of the maxima in the absorption spectrum between the wavelengths 2500 A and 4000 A (5.9). The wavelengths of some maxima in the absorption spectrum and minima in the excitation spectrum of crystalline Anthracene are also listed in Table V.

TABLE V

| Photoconduction wavelengths (5.9) | Excitation maxima | Excitation minima (1.4) | Absorption maxima (3.1) | Absorption maxima (5.15) |
|---|---|---|---|---|
| 3915 | 3120 | 3960 | 3910 | 3956 |
| 3700 | 3075 | 3740 | 3700 | 3920 |
| 3530 | 3005 | 3540 | 3510 | 3734 |
| 3420 | 2950 | 3370 | 3362 | 3702 |
| 3310 | 2860 | 3220 | | 3540 |
| 3140 | 2810 | | | 3374 |
| 3060 | 2760 | | | 2680 |
| 2960 | 2710 | | | 2600 |
| 2685 | (2650) | | | 2506 |
| 2590 | 2470 | | | 2404 |
| 2495 | | | | 2355 |
| 2370 | | | | |

Anthracene crystals are said to be photo-conducting i.e., a current will be conducted by the crystal if a voltage is applied between any two points on a section of the surface which is irradiated with ultra-violet light. If the wavelength but not the intensity of monochromatic ultra-violet light which illuminates the surface is varied, the current which flows will also vary. If the current which flows per unit intensity of the monochromatic light is plotted graphically as a function of the wave-length, the photo-conductivity spectrum of the crystal will be obtained.

As Anthracene absorbs ultra-violet radiation strongly (3.1, 3.2), the current conducted by the crystal will flow close to the surface through the molecules which absorb the radiation. The gaseous atmosphere surrounding the crystal greatly affects the intensity of the photo-conductivity spectrum. The intensity almost vanishes if the spectrum is measured when the crystal is surrounded by a rare gas or a vacuum, and it becomes relatively intense if the crystal is surrounded by air or oxygen (5.10).

It has been suggested that the photo-conductivity spectrum of an Anthracene crystal which has been prepared in a completely oxygen-free atmosphere, will vanish altogether (5.9). "In a molecular crystal such as Anthracene, there should be no large change in the properties of the molecules on the surface compared with those in bulk" (5.9, 5.11). It is also possible that the intensity of excitation spectra of Anthracene crystals prepared in a completely oxygen-free atmosphere will vanish altogether. Recently, evidence has been obtained to show that it is likely that the fluorescence spectrum of an Anthracene crystal is not characteristic of pure Anthracene, but may arise from "chemical agents" such as oxygen, or from

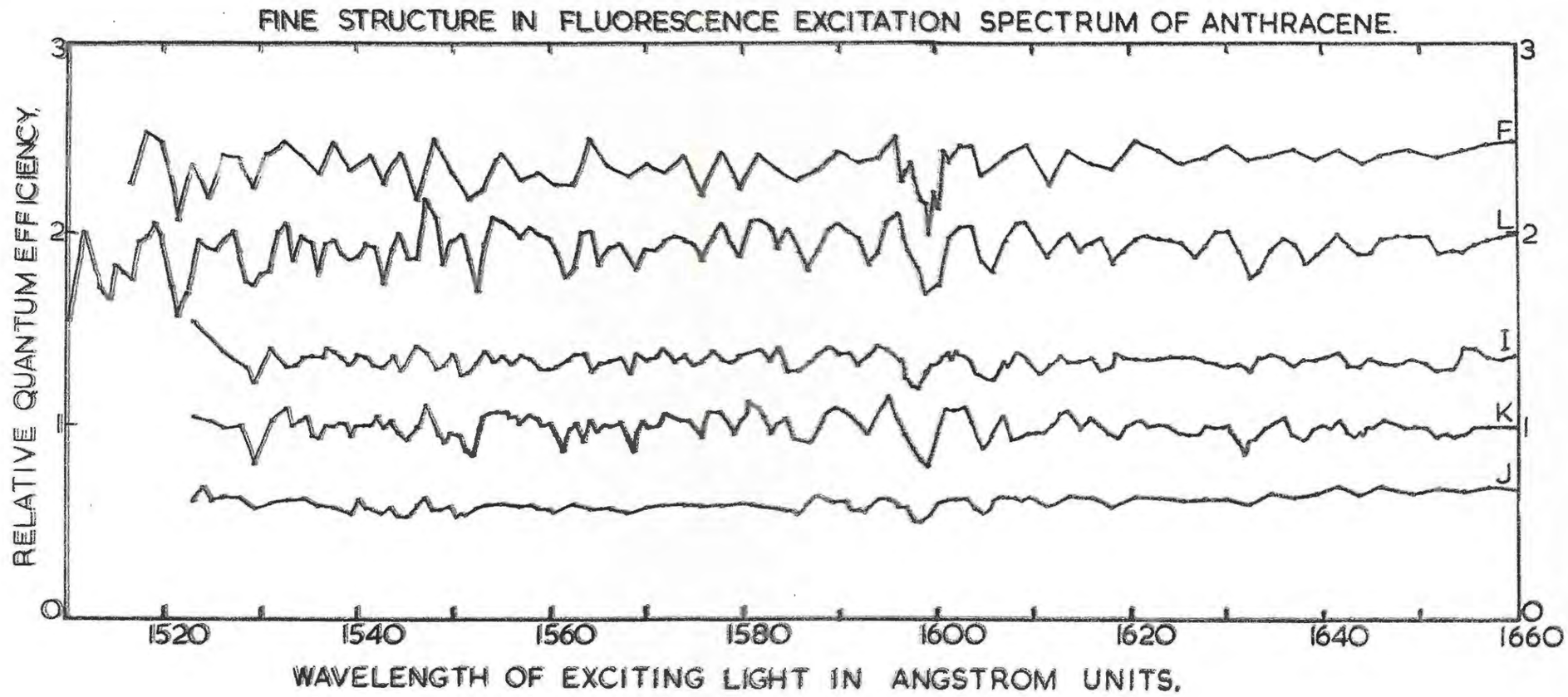
FINE STRUCTURE IN FLUORESCENCE EXCITATION SPECTRUM OF ANTHRACENE.
RELATIVE QUANTUM EFFICIENCY.
3
2
1
0
F
L
I
K
J
1520
1540
1560
1580
1600
1620
1640
1660
WAVELENGTH OF EXCITING LIGHT IN ANGSTROM UNITS.

DIAGRAM 5.5

imperfections in the crystalline lattice (5.8).

FINE STRUCTURE IN THE EXCITATION SPECTRUM:

Fine structure which was observed in the fluorescence excitation spectra of Anthracene crystals between the wavelengths 1510 A and 1650 A is illustrated in Diagram 5.5. (The spectra in Diagram 5.5 are sections of the spectra in Diagram 5.1). The wavelengths, wave numbers, and arbitrarily estimated relative intensities of the minima in the fine structure are given in Table VI. The wave numbers of the four most intense minima are listed in Table VII, and it would appear that the wave number spacings between these minima have a lowest common multiple of about 650 $cm^{-1}$. There appeared to be minima of slightly smaller intensity situated symmetrically one on either side of three of the four intense minima. It has been suggested that the fine structure is an interference phenomenon associated with the paths of "$\pi$" electrons around the "benzene rings" of the Anthracene molecules (5.12).

Although the excitation spectra in Diagram 5.5 are measured relative to Sodium Salicylate, the fine structure cannot be attributed to Sodium Salicylate. If the fine structure was characteristic of this chemical, the minima in the least intense spectra in Diagram 5.5 would be the most intense, and this is not observed to be the case.

TABLE VI

| $\nu$ ($cm^{-1}$) | $\lambda$ (A) | I | $\nu$ ($cm^{-1}$) | $\lambda$ (A) | I | $\nu$ ($cm^{-1}$) | $\lambda$ (A) | I |
|---|---|---|---|---|---|---|---|---|
| 60500 | 1653 | 2 | 62760 | 1593 | 4 | 64560 | 1549 | 2 |
| 60830 | 1644 | 2 | 63040 | 1586 | 6 | 64730 | 1545 | 3 |
| 61060 | 1638 | 3 | (63160) | (1583) | (1) | 64810 | 1543 | 2 |
| 61280 | 1632 | 5 | 63310 | 1579 | 3 | 64980 | 1539 | 1 |
| 61510 | 1626 | 3 | 63340 | 1576 | 2 | 65110 | 1536 | 3 |
| 61820 | 1618 | 2 | 63770 | 1568 | 3 | 65190 | 1534 | 2 |
| (61930) | (1615) | (1) | (63890) | (1565) | (1) | 65410 | 1529 | 7 |
| 62040 | 1612 | 4 | 64060 | 1561 | 4 | 65580 | 1527 | 2 |
| 62320 | 1605 | 5 | 64230 | 1557 | 1 | 65710 | 1522 | 10 |
| 62510 | 1599 | 10 | 64440 | 1552 | 5 | (65940) | (1516) | (3) |
| | | | | | | (66060) | (1514) | (7) |

TABLE VII.

| $\nu$ ($cm^{-1}$) | $\Delta\nu$ |
|---|---|
| 61280 | |
| | 1330 |
| 62510 | |
| | 1930 |
| 64440 | |
| | 1270 |
| 65710 | |

DIFFERENCES BETWEEN THE EXCITATION SPECTRA OF A GIVEN CRYSTAL:

The (001) spectra of cleaved crystals were more intense than the (010) or (1'00) spectra.

e.g.:- Compare the intensity of the (001) spectrum F with the intensity of the (1'00) spectrum L, and of the (010) spectrum I in Diagram 5.4.

(It should be noted that the zero of the ordinate scale for curve I is .6 unit above the zero on the diagram). The surfaces obtained by cleavage of the (001) faces of Anthracene crystals were always very smooth compared with surfaces obtained by cleavage of other faces of the crystals, and possibly the smoothness of surfaces influences the fluorescent intensity. The crystals appeared more translucent in a direction perpendicular to the (001) planes, than in other directions. When excitation spectra were measured, fluorescence passed through the crystal before reaching the photo-multiplier tube, and possibly a greater intensity of fluorescence reached the photo-multiplier when the (001) spectra were measured than when the other spectra were measured.

If the (001) spectrum F in Diagram 5.4 is compared with the (1'00) spectra J, K and the (010) spectrum I, it will be observed that the two minima at the wavelengths 1910 A and 2220 A hardly appear in the (001) spectrum. The wavelength of the intense maximum in the excitation spectrum of a particular crystal occurred at a larger wavelength in the (010) spectrum than in either the (1'00) or (001) spectra

e.g.:- Compare curve I, Diagram 5.4, with curves F and L.

The surface of the crystal on which the exciting radiation fell had been rubbed with a cloth before the measurement of curve I, and it was possibly the rubbing which caused the maximum in the (010) spectrum to occur at a longer wavelength. Also, minima in the fine structure appeared to be more intense in the (1'00) spectra than in either the (010) or (001) spectra.

e.g.:- Compare the (1'00) spectra K and L in Diagram 5.5 with the (010) and (001) spectra I and F of cleaved crystals.

(It should be noted that the zero of the ordinate scale for curve L is .6 unit above the zero on the diagram). As explained in Chapter III, the normals to the planes of the molecules in the lattice made a smaller angle with the direction of the exciting light when the (1'00) spectra were measured than when either the (010) or (001) spectra were measured, and this fact might account for the greater depth of the minima in the fine structure. It was not possible to find a satisfactory correlation between all the differences in the spectra and the orientation of the planes of the molecules with respect to the direction of the exciting light. Investigation of these differences in the excitation spectra measured using polarised exciting light might give interesting results, for the strength of absorption of polarised ultra-violet light by Anthracene crystals has been found to depend on the angle which the plane of polarisation makes with axes in the planes of molecules in the crystals (3.2).

THE FIRST IONISATION POTENTIAL:

It was observed that the intensities of the fluorescence excitation spectra of Anthracene are independent of wavelength between 1500 A and

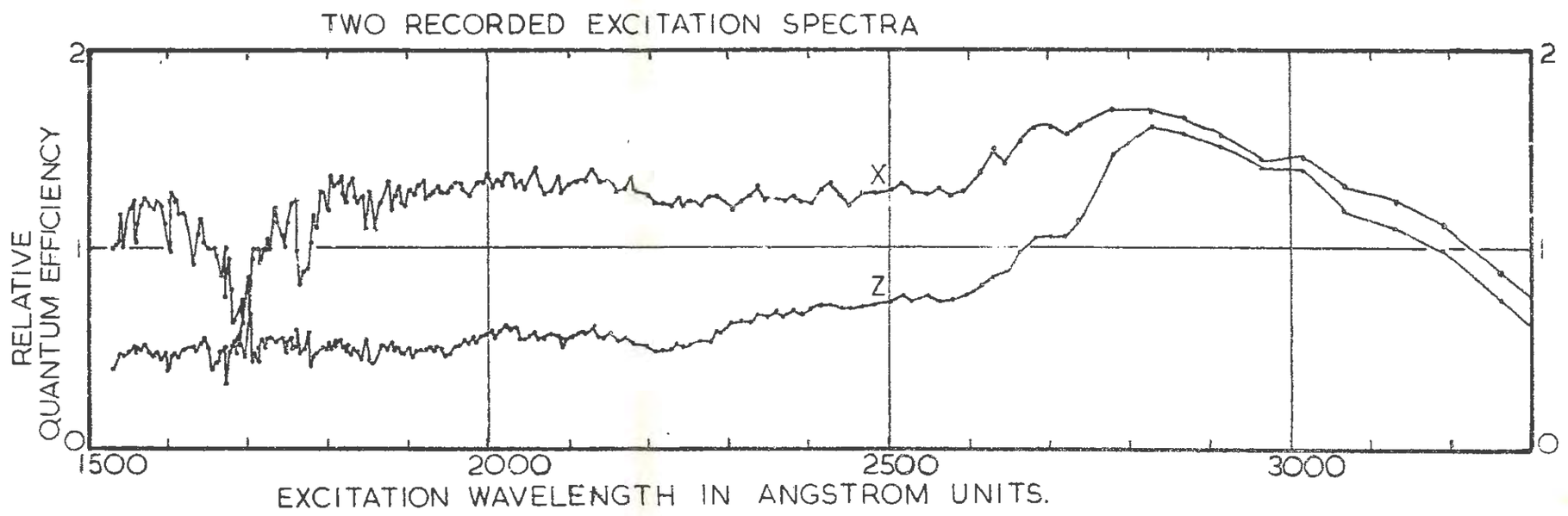
TWO RECORDED EXCITATION SPECTRA
RELATIVE QUANTUM EFFICIENCY
2
1
0
X
Z
1500
2000
2500
3000
EXCITATION WAVELENGTH IN ANGSTROM UNITS.

DIAGRAM 5.6

1650 A (neglecting variations in intensity caused by the fine structure). The wavelength at which the intensities of the spectra become independent of wavelength is about 1650 A (See Diagram 5.1). The ionisation potential of Benzene is associated with the wavelength at which the absorption spectrum becomes intense and independent of wavelength (5.13). As Anthracene is closely related in chemical structure to Benzene, it is likely that the ionisation potential of Anthracene is associated with the wavelength at which the Anthracene absorption spectrum becomes intense and independent of wavelength.

The fluorescence excitation spectrum of crystalline Anthracene varies in an inverse way to absorption spectrum near the wavelengths 2200 A and 1890 A, and if the excitation spectrum still varies inversely to the absorption spectrum at shorter wavelengths, the wavelength 1650 A might be associated with the ionisation potential of Anthracene. The energy of a quantum of radiation having a wavelength 1650 A is 7.5 eV., and the ionisation potential of Anthracene has been estimated theoretically to be 7.23eV (5.14). It is possible that the presence of surface oxides on Anthracene crystals would affect the value of the ionisation potential estimated from the excitation spectra.



AN UNUSUAL EXCITATION SPECTRUM:

The two excitation spectra of Anthracene crystals illustrated in Diagram 5.6 were measured simultaneously, and it was found difficult to account for three minima in the more intense curve. It was recalled that the surface of one of the crystals had been wiped with cotton wool soaked

in Acetone before measurement of the spectra, and it is possible that Acetone adsorbed on the surface caused the appearance of the minima, the wavelengths of which are estimated as 1850 A, 1760 A, 1680 A.

EXCITATION SPECTRA:

When a beam of radiation falls on a slab of material, the energy of the beam which is neither transmitted nor reflected by the slab may be absorbed and converted to heat. If the radiation excites luminescence of the material, some of the energy of the beam can be converted to fluorescence and phosphorescence as well as heat. At the wavelength of a maximum in the absorption spectrum, there may be a maximum or a minimum in the fluorescence excitation spectrum, depending on whether a greater fraction of the exciting radiation is converted to fluorescence, or to heat (and phosphorescence). Minima in the excitation spectrum at wavelengths 1910 ± 10 A, 2220 ± 12 A, and a maximum at the wavelength 2710 ± 20 A coincide closely with maxima in the absorption spectrum at the wavelengths 1890 A, 2200 A and 2680 A (3.2, 5.1, 5.15).

Two distinguishable luminescences, namely fluorescence and phosphorescence, can be observed when (Anthracene) molecules are excited by ultraviolet radiation (5.16). (Most of the wavelengths of the fluorescence spectrum occur in the vizible region, and the wavelengths of the phosphorescence spectrum occur in the infra-red region of the electromagnetic spectrum).

The intensity of the phosphorescence of Anthracene is usually weak compared to the intensity of fluorescence (1.8). Some of the excited molecules, instead of returning directly to the ground state with the emission of fluorescence, may pass into the "phosphorescent" or "triplet" state, and may then return to the ground state with the emission of phosphorescence (5.17). Molecules in the phosphorescent state may also return to the ground state without the emission of phosphorescence, so that it is possible for all the energy which excites an (Anthracene) molecule to be lost without the emission of luminescence (5.17).

Different wavelengths of ultra-violet light will excite molecules from the ground state to different vibrational levels of the first and higher excited states. If the probability of an excited molecule passing to the phosphorescent state depends on the vibrational level to which the molecule has been excited (i.e., depends on the energy of exciting radiation), variations in the fluorescence excitation spectrum might be expected. Molecules in the first excited state may pass to the triplet state when a mixing of vibrational levels of the two states occurs (5.17).

The fluorescence excitation spectra of single Anthracene crystals are different from those of microcrystalline layers of Anthracene, in that the spectra of microcrystalline layers are almost independent of wavelength (3.4, 5.18). The difference between the spectra might suggest that variations in the fluorescence excitation spectra with wavelength only appear when the Anthracene molecules are in a state of order.

The difference between the spectra might also be connected with the fact that the fluorescence [redacted] spectra of microcrystalline layers extend to shorter wavelengths than the fluorescence spectra of single crystals (5.19). It was explained in Chapter I that the excitation spectra of solutions are independent of wavelength, and the molecules in solution would not be in a state of order.

SUGGESTIONS IN CONCLUSION:

Measurements of the fluorescence excitation spectra of Diathracene, oxides and peroxides of Anthracene, and of other materials having the property of fluorescence might give interesting information about fluorescence excitation spectra.

Measurements of phophorescence excitation spectra should be made. It is suggested that maxima in the fluorescence excitation spectra might correspond to minima in the phosphorescence excitation spectra (and vice-versa).

A method of measuring ultra-violet absorption spectra of non-fluorescent substances is suggested. If a very thin layer of a non-fluorescent substance is coated on the surface of a fluorescent crystal, the fluorescence excitation spectrum, measured when the exciting light falls on any section of the coated surface of the crystal should have the inverted absorption spectrum of the non-fluorescent substance superimposed on it.

# BIBLIOGRAPHY.


| | | | |
|---|---|---|---|
| 1.1 | Platt, C.M. | : | A new monochromator for the vacuum ultra-violet. Thesis. Rhodes University, 1959. |
| 1.2 | Stepanov, B.I. | : | Vavilov's Law. Uspekhi Fiz. Nauk. 58 3-36, 1956. |
| 1.3 | Wright, G.T. | : | Proc. Phys. Soc. B. 68 241, 701, 1955. |
| 1.4 | Wright, G.T. | : | Phys. Rev. 100 587, 1955. |
| 1.5 | Johnson, F.S., Watanabe, K. & Tousey, R. | : | J. Opt. Soc. Am. 41 702-8, 1951. |
| 1.6 | Pringsheim, P. | : | Fluorescence and Phosphorescence. Interscience Publishers, 1949. |
| 1.7 | Birks, J.B. | : | Energy transfer in organic phosphors. Phys. Rev. 94 1567, 1954. |
| 1.8 | Birks, J.B. | : | Scintillation Counters. Pergamon, p.67, 1953. |
| 1.9 | Bowen, E.J. & Wokes, F. | : | Fluorescence of solutions. Longmans, p.43, 1953. |
| 1.10 | Vavilov, S.I. | : | Z.f. Physik 42 311, 1927. |
| 1.11 | Antonov Romanovsky, V.V. | : | J. Phys. Radium 17 694, 1956. |
| 2.1 | Tousey, R. & Hass, G. | : | J. Opt. Soc., Am. 49 593, 1959. |
| 2.2 | Landolt-Börnstein Tables. 4th Edition. Bec. 209, 969, 1912. | | |
| 2.3 | Ditchburn, R.W. | : | Opt. Acta. 3 No. 2, 1956. |
| 3.1 | Kortüm, G. & Finckh, B. | : | Z. Phys. Chem. B.52. 263, 1942. |
| 3.2 | Craig, D.P. & Hobbins, P.C. | : | J. Chem. Soc. 2309, 1955. |
| 3.3 | Watanabe, K. & Inn, E.C.Y. | : | J. Opt. Soc. America 43 32-5, 1953. |

3.4 Hammann, J.F. : Z.f. Angew. Phys. 10 187-92, 1958.

3.5 Clarke, F.J.P. & Garton, W.R.S. : J. Sci. Instruments 36 408, 1959.

3.6 Berton, A. : Comptes Rendus 208 1898-1900, 1939.

3.7 Origin unknown : Microfilm at Physics Department, Rhodes University.

3.8 Wood, R.W. : Physical Optics. MacMillan, 3rd Edition, 1934.

3.9 Sinclair, V.C. et al: Acta Cryst. 3 251, 1950.

3.10 Lyman, Th. : Spectroscopy of the extreme ultra-violet. Longmans, 1914.

4.1 Handbook of Chemistry and Physics. Chem. Rubber Pub. Co. 33rd Edition, 1951 - 52.

4.2 Fowles, G.R. : Phys. Rev. 78 745, 1950.

4.3 Shenstone, A.G. : Phil. Trans. Roy. Soc. London 235 195, 1936.

5.1 Lyons, L.E. : J. Chem. Phys. 23 1973, 1955.

5.2 Lipsett, F.R. et al: J. Chem. Phys. 26 1444, 1957.

5.3 Karyakin, A.V. & Terenin, A.N. : Izv. Akad. Nauk. USSR. Ser. Fiz. 13 4-17, 1949.

5.4 Capper, A. & Marsh, J.K. : J. Am. Chem. Soc. 47 2847, 1925.

5.5 Nechaeva, N.E. et al: Zh. Eks. Teor. Fiz. USSR. 22 380-1, 1952.

5.6 Bree, A. & Lyons, L.E. : J. Chem. Physics. 384 1956.

5.7 Miller, J.A. & Baumann, C.A. : J. Am. Chem. Soc. 65 1540 1943.

5.8 Solid State Physics. (Seitz, F. and Turnbull, D.) H.C. Wolf 9 55 Academic Press, 1959.

5.9 Bree, A., Carswell, D.J. & Lyons, L.E. : J. Chem. Soc. 1728, 1734 1955.

| | | | |
|---|---|---|---|
| 5.10 | Chynoweth, A.G. | : | J. Chem. Phys. 22 1029-32, 1954. |
| 5.11 | Davydov, A.S. | : | Izv. Akad. Nauk. USSR 14 502, 1950. |
| 5.12 | Archer, S. | : | Rhodes University, Grahamstown, 1960. |
| 5.13 | Wilkinson, P.G. | : | Canad. J. Physics 34 596, 1956. |
| 5.14 | Matsen, F.A. | : | J. Chem. Phys. 24 602, 1956. |
| 5.15 | Obreimov, I.V. & Prikhotko, A. | : | Phys. Z. Sov. Union 1 203, 1932. 9 34, 1956. |
| 5.16 | Kasha, M. | : | Chem. Rev. 41 401, 1947. |
| 5.17 | Rosenberg, B.J. | : | J. Chem. Phys. 29 1108, 1958. |
| 5.18 | Galanin, M.D. & Chizhikova, Z.A. | : | Zh. Eks. Teor. Fiz. 26 624, 1954. |
| 5.19 | Birks, J.B. & Wright, G.T. | : | Proc. Phys. Soc. London, B67 657 1954. |

OF CRYSTALLINE ANTHRACENE

by

A. S. DRIVER B.Sc. Hons (Rhodes)

---

## SUMMARY OF CONTENTS.

In Chapter I, the terms "quantum efficiency" and "fluorescence excitation spectrum" are defined. Previous work on the fluorescence excitation spectrum of single Anthracene crystals is briefly summarised, and the purpose of the investigations undertaken in the course of the research is stated. The writers Pringsheim and Bowen believe that the intensities of fluorescence excitation spectra become independent of wavelength when certain corrections are applied to the spectra. Theories developed as a consequence of this belief, by Pringsheim and Birks, are described.

In Chapter II, there is given a description of a prism spectrograph constructed for use in the vacuum ultra-violet region of the spectrum. The dispersion of the spectrum at various wavelengths is calculated.

In Chapter III, the method of measurement of fluorescence excitation spectra is explained. By means of an attachment to the spectrograph, it is possible to cleave an Anthracene crystal inside the evacuated interior of the spectrograph, so that fluorescence excitation spectra of crystals can be measured in such a way that the radiation exciting fluorescence falls on a newly cleaved face, not yet exposed to the atmosphere. In agreement with the results of other workers, differences between the fluorescence excitation spectra of

Sodium Salicylate layers of different thicknesses are observed. A method for identifying the crystallographic planes of Anthracene is described, and the possible effects of the spectral variation of the reflectivity of Anthracene on the fluorescence excitation spectrum is discussed. The spectrum obtained from a Hydrogen capillary discharge tube is found to be similar to the same spectrum measured by workers using other types of spectrograph.

In Chapter IV, the method of calibrating the spectrograph in terms of the wavelengths of identifiable spectrum lines is described. Details are given of the construction of a Schüler hollow-cathode discharge tube used for exciting lines having wavelengths in the vacuum ultra-violet region of the spectrum.

In Chapter V, measurements of fluorescence excitation spectra of Anthracene crystals, and deductions from the measurements are given. The results suggest that the fluorescence excitation spectrum of crystalline Anthracene is essentially a surface phenomenon, and evidence is obtained to strengthen the view that fluorescence is not a property of pure Anthracene molecules. The first ionisation potential of Anthracene is estimated from the spectra, and fair agreement is obtained with a value determined theoretically by

fluorescence excitation spectrum at wavelengths corresponding to energies greater than the ionisation potential, and the wavelengths of about thirty minima in the fine structure are tabulated. A possible qualitative explanation of variations in the intensity of fluorescence excitation spectra with wavelength is proposed. Problems requiring investigation are suggested, and also a method for measuring absorption spectra of non-fluorescent compounds.

----- oOo -----